UNIVERSITY OF NAPLES "FEDERICO II"

DOCTORATE SCHOOL IN
MOLECULAR MEDICINE AND MEDICAL BIOTECHNOLOGY
XXIX CYCLE

RESISTANCE OF CANCER CELLS TO PHOTODYNAMIC THERAPY WITH 5-AMINOLEVULINIC ACID: ROLE OF THE ABCG2 TRANSPORTER

TUTOR

Prof. Giuseppe Palumbo

Prof. Vittorio Enrico Avvedimento

CANDIDATE

Dr. Federica Barra

COORDINATOR

Prof. Vittorio Enrico Avvedimento

ACADEMIC YEAR 2015/2016

“[…]καὶ τάχα δὴ ἀκούουσι βοώντων τῶν στρατιωτῶν
‘θάλαττα θάλαττα’ […]”
Senofonte

To my parents,

To “DSB Group” unique, unrepeatable and irreplaceable,

To Annalisa and Ilaria, my models of women, mothers and scientists.

LIST OF ABBREVIATIONS

5-ALA	5-Aminolevulinic acid
5-ALA/PDT	Photodynamic Therapy with 5-Aminolevulinic acid
ABCG2, B1 and C1	ATP binding cassette transporter G2, B1 and C1
ATM	Ataxia-Telangiectasia Mutated protein
BCRP	Breast Cancer Resistant Protein
DMSO	Dimethyl sulfoxide
FDA	Food an Drug Administration
HAL	Hexyl aminolevulinate
HpD	hematoporphyrine derivatives
ISC	Intersystem crossing
MAL	Methyl aminolevulinate
MDR	Multi Drug Resistance
mRNA	messenger RNA
PBGD	Porphobilinogen deaminase
PDT	Photodynamic Therapy
PpIX	Protoporphyrin IX
PS	Photosensitizer
ROS	Reactive oxygen pecies

TABLE OF CONTENTS

LIST OF PUBLICATIONS

The main body of this Thesis is based upon the following publication:

Postiglione I[†], **Barra F**[†], Aloj SM, Palumbo G. "Photodynamic therapy with 5-aminolaevulinic acid and DNA damage: unravelling roles of p53 and ABCG2". *Cell Prolif.* **2016** Aug;49(4):523-38. doi: 10.1111/cpr.12274.

[†] **= equal contribution**

I kindly thanks *Cell Proliferation*'s editors for their license about figures and parts of the text.

Other Publications:

Pollio A, Zarrelli A, Romanucci V, Di Mauro A, **Barra F**, Pinto G, Crescenzi E, Roscetto E, Palumbo G. "Polyphenolic Profile and Targeted Bioactivity of Methanolic Extracts from Mediterranean Ethnomedicinal Plants on Human Cancer Cell Lines". *Molecules.* **2016** Mar 23;21(4):395. doi: 10.3390/molecules21040395.

Barra F, Roscetto E, Soriano AA, Vollaro A, Postiglione I, Pierantoni GM, Palumbo G, Catania MR. "Photodynamic and Antibiotic Therapy in Combination to Fight Biofilms and Resistant Surface Bacterial Infections". *Int J Mol Sci.* **2015**; 16(9):20417-30. doi: 10.3390/ijms160920417.

Postiglione I, Chiaviello A, **Barra F**, Roscetto E, Soriano AA, Catania MR, Palumbo G, Pierantoni GM8. " Mitochondrial Malfunctioning, Proteasome Arrest and Apoptosis in Cancer Cells by Focused Intracellular Generation of Oxygen Radicals". *Int J Mol Sci.* **2015**; 16(9):20375-91. doi: 10.3390/ijms160920375.

ABSTRACT

Photodynamic Therapy (PDT) is a minimally invasive radiation therapy currently used in treatment of various cancerous and pre-malignant diseases.

Photodynamic therapy with 5-aminolaevulinic acid (5-ALA/PDT) induces DNA damage following photoactivation of Protoporphyrin IX (PpIX), the photosensitizer generated from the endogenous metabolism of 5-ALA. The occurrence of DNA damage could represent one of the last causes of cell death induced by PDT.

We have dissected the molecular effectors involved in the DNA damage induced by 5-ALA/PDT in several cell lines: 1. two lung adenocarcinoma cell lines, namely H1299 ($p53^{-/-}$) and A549 wild type ($p53^{+/+}$); 2. two sub-clones of the same cell line HCT-116, that differ for p53 expression ($p53^{+/+}$ and $p53^{-/-}$) and 3. a prostate adenocarcinoma cell line, PC3 ($p53^{-/-}$). We have focused our attention on p53, which controls the DNA damage response and on the efflux regulator ATP binding cassette transporter G2 (ABCG2). The levels and the activity of these two gene products are relevant for the survival in cells exposed to photodynamic treatment. Cell cycle, DNA damage (phosphorylated γ-H2AX and Comet assay) and ABCG2 levels were measured before or after irradiation.

We found that all cell lines, except A549 and PC3, underwent extensive DNA damage upon PDT. The resistance of A549 and PC3 cells to photodynamic DNA damage was due to the high levels of ABCG2 expression upon irradiation. In fact, these cells displayed high levels of DNA damage signatures and underwent death when the ABCG2 was inhibited. Analysis of ABCG2 expression shows a complex regulation at transcriptional and post-transcriptional levels and its expression was dependent on oxidative stress. On the other hand, p53 expression or activity did not exert a significant effect on 5-ALA-induced cell death.

Taken together, all these findings provide novel information on the role of the ABCG2 transporter in oxidative stress and a new tool to manipulate resistance to photodynamic therapy.

1. INTRODUCTION

1.1 BACKGROUND INFORMATIONS

Photodynamic Therapy (PDT) is a photochemistry-based therapeutic approach that requires the employ of a non-toxic Photosentitizers (PS), a light source specific for the selected PS and oxygen presents into cells' microenvironment.

After the systemic administration of a non-toxic PS (generally, an exogenous molecule), the PS accumulates in host and tumor cells (FIGURE 1). The subsequent illumination of the tumor site with the light source, corresponding to the specific PS absorption wavelength, excites the PS and leads to the generation of singlet oxygen and other reactive oxygen species (ROS), which caused oxidative damage to intracellular macromolecules and consequently leads cells to death[1].

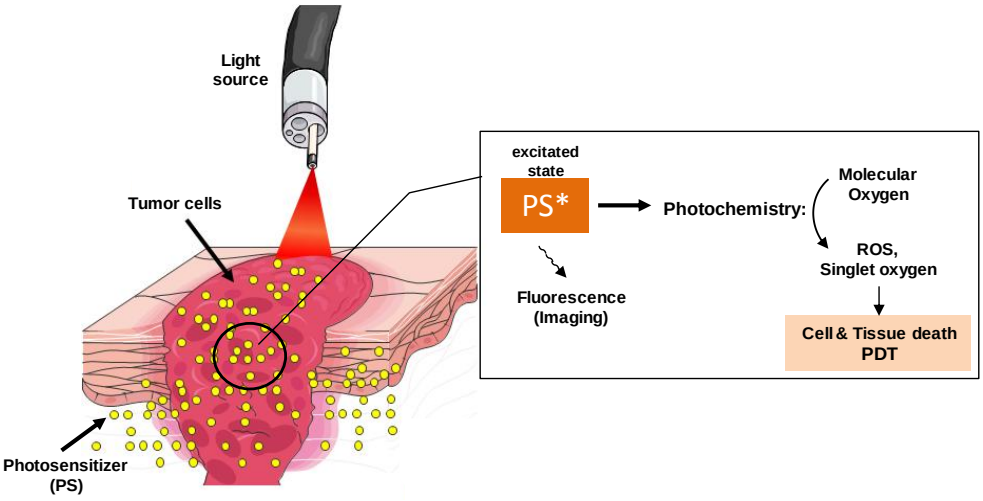

FIGURE 1. Basic principle of Photodynamic Therapy (PDT).

Despite several advantages, Photodynamic therapy remains a marginal approach to cure specific types of cancers mainly because the low penetration of light into human tissues. This limited penetration into targeted tissue prevents the occurrence of an efficient stimulation of the PS in tumor lower layers except those directly illuminated (i.e. the very first, approximately 2 mm into the tissue which is sufficient in many cases for skin diseases) or those just under them. Depending on the selected PS, the effects of irradiation can reach since 1-1,5 cm into tissue and internal solid tumors can be reached by interstitial optics fiber or scopes[2,3].

Generally, the damage mediated by ROS occurs at the site of accumulation of the PS and cells death is induced by a mixture of apoptosis, necrosis and autophagy. PDT may or may not induce DNA damage due to ROS propagation, half life of the species generated and ability to cells to retain them[4]

1.2 STORY OF PHOTODYNAMIC THERAPY

The therapeutic properties of light were approved for clinical trials only in the last century but the use of the light as a treatment for diseases has a very ancient origin. In fact, it is known that light has been used as therapy for more than three thousand years as Egyptian, Indian and Chinese civilizations used light to treat various diseases, in general skin cancers[5].

At the beginning of the twentieth century, Niels Finsen developed "phototherapy" to treat diseases. He used red-light exposure to prevent the formation and release of smallpox pustules and the ultraviolet light from the sun to treat cutaneous tubercolosis. Such treatments introduces the era of the modern light therapy and, for his discoveries, Finsen won the Nobel prize in Physiology or Medicine in 1903[6] (FIGURE.2).

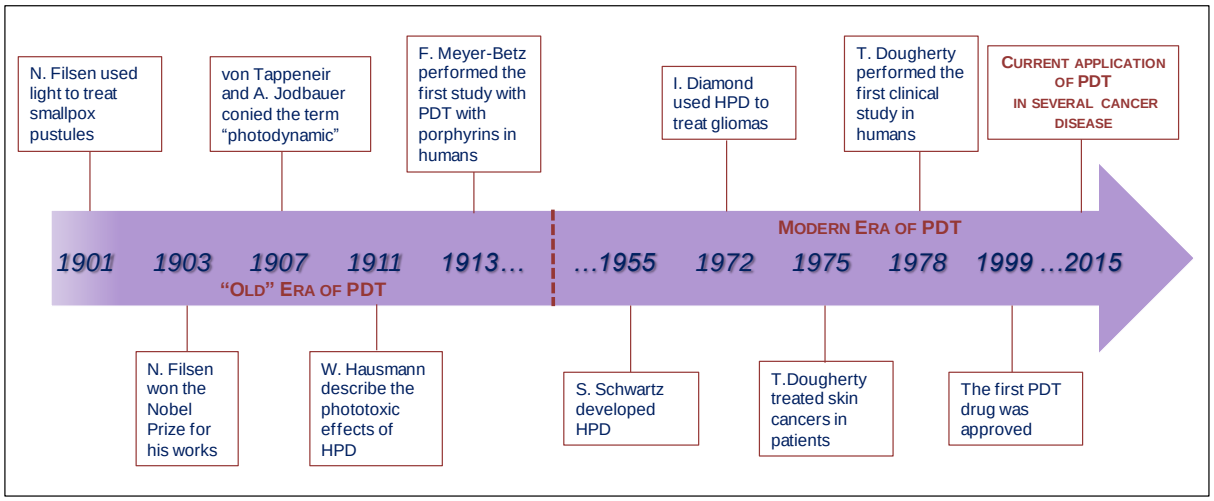

FIGURE 2. Timeline of selected milestones in the historical development of PDT (2015).

From these experiments, the therapeutic application of PDT *in vivo* and on patients took a long time. We have to wait the 1975, when T. Dougherty and his co-workers succeeded in completely eradicating mammary tumor growth in mice[7]. Following these preliminary successes, in 1999 the Food and Drug Administration (FDA) approved the first PDT drug in Canada. The photosensitizer was Photofrin®, a partially purified HpD, discovered by

Dougherty in 1983[8] and also nowadays is still the most commonly used photosensitizer in clinical use.

After Photofrin®, new photosensitizers were developed and the most common ones approved for clinical use are Foscan (a chlorine photosensitizer), 5-aminolevulinic acid (5-ALA, Levulan®) and 5-ALA methylesther (Metvix).

Currently, PDT is recommended for patients with early-stage dermatological cancers that were inoperable and, more in general, for the treatment of non malignant, malignant and pre-malignant diseases localized in hollow organs achievable by a light probe[1] (TABLE 1)

DRUG	COUNTRY	DISEASE
		NON-MALIGNANT
Visudyne	EU, USA	AMD – age-related macular degeneration
Methylene Blue	EU	Periodontitis
		PRE-CANCER
Levulan, Metvix	EU	Actinic keratosis Non-Melanoma skin cancer
Photofrin	EU, USA	Barret's oesophagus
Photofrin, Hexvix	Japan	Cervical dysplasia
		CANCER
Metvix	EU	Basal-cell carcinoma
Photofrin; Hexvix, Levulan	Japan	Cervical cancer
Photofrin	Canada, Denmark, Finland, France, Germany, Ireland, Japan, The Netherlands, UK, USA	Endobroncheal cancer
Photofrin	Canada, Denmark, Finland, France, Ireland, Japan, The Netherlands, UK, USA	Oesophageal cancer
Photofrin	Japan	Gastric cancer
Foscan	EU	Head and neck cancer
Photofrin	Canada	Papillary bladder cancer
Tookad	EU	Prostate cancer
Hexvix	EU	Bladder cancer (fluorescence guided resection)
5-ALA	EU, Japan	Glioblastoma (fluorescence guided resection)

TABLE 1. Types of disease and cancer treated with PDT and approved drugs (2015).

1.3 PRINCIPLES AND PHOTOCHEMISTRY OF PHOTODYNAMIC THERAPY

PDT exerts its therapeutic effects through the oxygen present in the cell microenvironment. The photochemical reaction that generates singlet oxygen from the ground-state oxygen is represented by the Jablonsky diagram (FIGURE 3).

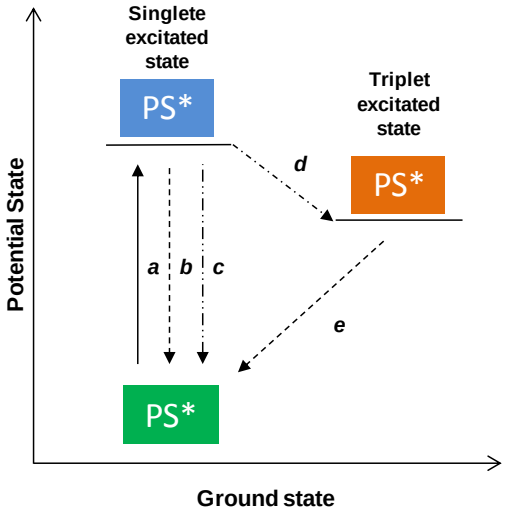

FIGURE 3. Jablonski diagram showing the various modes of excitation and relaxation in a photosensitizers: *a.* excitation, *b.* fluorescence, *c.* non-radiative decay, *d.* intersystem crossing (ISC), *e.* phosphorescence.

After irradiation, the PS from the ground-state is transformed into a transient excited state. When it returns into its ground-state, the energy relapsed can be transformed into a fluorescent signal or, more interesting, can be converted into an excited triplet state via intersystem crossing (ISC)[9]. From this state, the PS can also return into its ground state by emitting a phosphorescent photon or giving rise to two types of reactions referred to as type I and II (FIGURE 4).

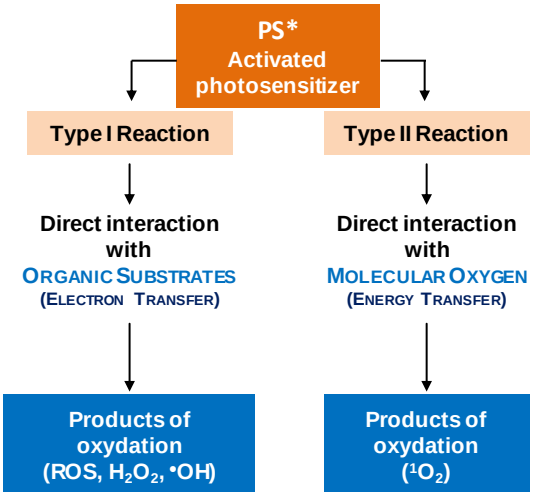

FIGURE 4. Schematic representation of Type I and Type II reaction in PDT.

In type I photoreaction, the excited photosensitizer transfers one electron to a substrate causing the formation of radical species (radical or ion-radical), which, in the presence of oxygen, yield reactive oxygenated products. Alternatively, the direct transfer of the extra electron to oxygen generates a superoxide radical anion. In the type II reaction, the excited sensitizer may form excited state singlet oxygen ($^1O_2$) by transferring its excess energy to ground-state molecular oxygen. Singlet oxygen, then, reacts with the substrate to generate oxidized products. Generally, Type II reactions are predominant in PDT although both reactions can occur simultaneously inside the cells. Moreover, the photosensitizer is not destroyed through this process but become inactive through a photochemical process called photobleaching, by which the PS can be transformed into a different molecular form that does not absorb light[10, 11].

1.4 PHOTOSENSITIZERS IN CLINICAL PDT

The ideal photosensitizers in clinical PDT, both of natural or synthetic origin, must have specific characteristics. It must not be a toxic chemical, it should be selective and should accumulate in those tissues where it can be useful. Its wavelength absorption must not interfere with other chromophores present within cells and tissues but must be also excitable at longer wavelengths of activation for a deeper tissue penetration. Moreover, it must have an easy administration, a suitable solubility in cell's microenvironment and a high accessibility for target cells[12].

Current available photosensitizers can be categorized into various and broad families: the hematoporphyrins and its derivatives (HpD), the chlorins and the dyes.
Among these, most of the PSs used in cancer therapy are HpD and, in particular, Photofrin® (a mixture of mono-, di- and oligomers that all contain a porphyrin moiety) is the most commonly administered in fact is still nowadays used for the treatment of bladder cancer, esophageal cancer, early non-small cell lung cancer and Barrett's esophagus. Unfortunately, although it succeeded in fighting such types of cancers, there are several limitations of its use. First, it is composed by a mixture of about 60 compounds so its composition is difficult to reproduce. Moreover, high concentrations of both PS and light must be administered to the patients with the drawback that it is also not very selective for tumor tissue[1].
So, it was necessary to invest significative efforts in the development of new photosensitizers.

1.5 5-AMINOLEVULINIC ACID: A PRODRUG FOR PDT

5-aminolevulinic acid (5-ALA, FIGURE. 5) is not considered a PS *per se* due to the fact that it is the precursor of the natural photosensitizer protoporphyrin IX (PpIX). It is a polar molecule and, in physiological pH, occurs mainly as a charged zwitterion. Such characteristic account for its low lipid solubility and reduced bioavailability.

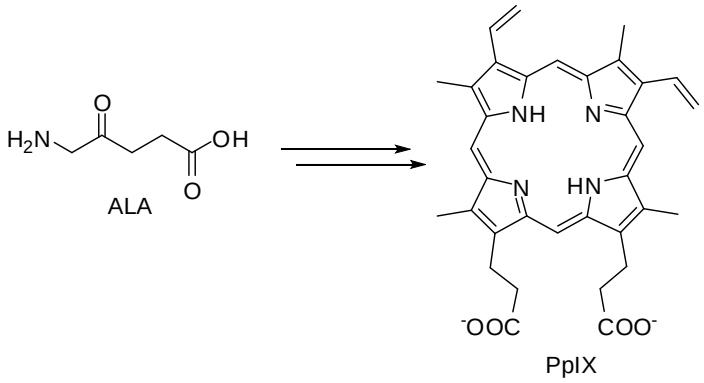

FIGURE 5. 5-Aminolevulinic Acid (5-ALA), the precursor of natural PS protoporphyrin IX (PpIX).

Once inside the cells, 5-ALA is metabolized by the heme biosynthetic pathway where in 7 step is transformed into PpIX, the real PS. In the physiological pathway, PpIX is transformed into heme by the action of the enzyme ferrochelatase that binds an iron atom to PpIX to form heme. The production of heme exerts a normal feedback repression on the enzyme ALA

synthase, that is the regulatory enzyme of the all pathway[13] (it is also important to note that such enzyme can be repressed not only by a direct inhibition but also by inhibiting its transcription, translation and transport into mitochondria[14]). It is known that, although nearly all human cell types are able to produce heme due to the presence of the enzymes involved in the synthetic pathway, a distinct activity of the enzymes in tumor leads to a higher PpIX accumulation within transformed cells.[15] In fact, in such cells, there is a decreased activity of ferrochelatase[16, 17], an higher activity of porphobilinogen deaminase (PBGD, that catalyzes the formation of uroporphyrinogen III from porphobilinogen)[14] and a limited availability of iron[18] therefore, by administering 5-ALA exogenously in large excess, an higher amount of PpIX accumulates inside the cells that became photosensitive (FIGURE. 6).

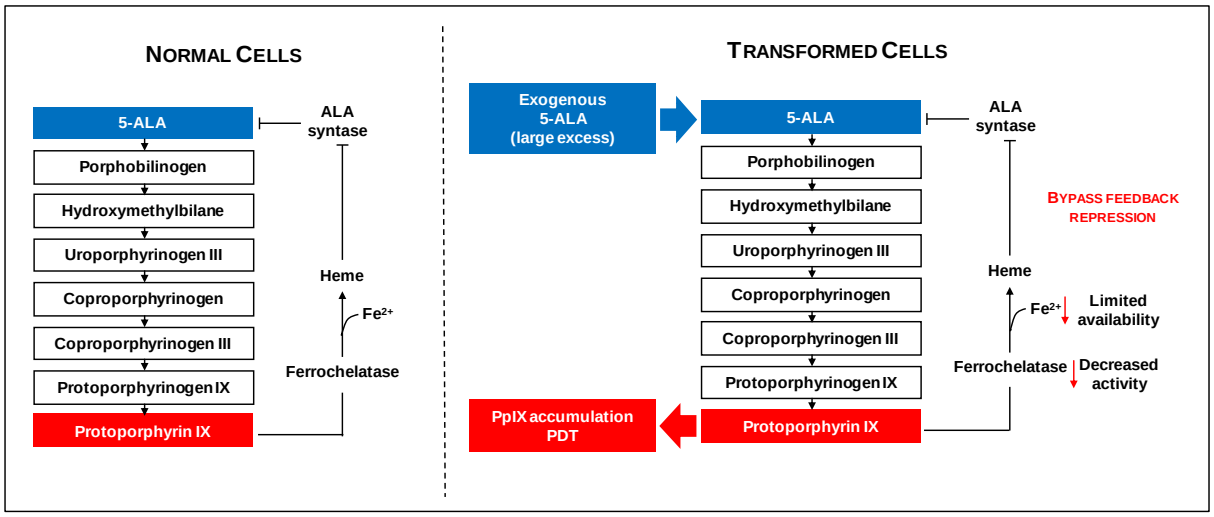

FIGURE 6. Schematic representation of heme biosynthesis in normal and transformed cells.

Thanks to its prodrug characteristics, 5-ALA is considered a good molecule for PDT because represent an alternative approach to the direct administration of a PS. In fact, it is administered topically so it is possible to localize the treatment course without burning the untreated regions.

5-ALA also presents some limits like a low lipophilicity and a scarce membrane and skin permeability. To this purpose, an improvement of the compound takes advantages from several modifications at its carboxyl termination. Until now, at least 77 various 5-ALA modifications have been reported. The most successful 5-ALA derivatives are its esters: methyl ester (methyl aminolevulinate, MAL, Metvix®) and hexyl ester (hexyl

aminolevulinate, HAL, Hexvix®). Elongation of a carbon chain attached to 5-ALA results in increased lipophilicity and, in consequence, higher membrane and skin permeability[19].
The very first topical application in the clinical use of 5-ALA/PDT was in 1990[19] for the treatment of basal cell carcinoma and, since that moment, the use of 5-ALA/PDT is still growing. Nowadays, 5-ALA/PDT is an approved treatment for several cancer diseases such as actinic keratosis[20], superficial bladder cancers[21], gliomas[22], gastric cancers[23] and non-melanoma skin cancer[24].
All these evidences make 5-ALA and its derivatives a versatile and efficient therapeutic strategy, with a broad field of application.

1.6 PHOTODYNAMIC THERAPY AND DNA DAMAGE

Compared to the other traditional cancer therapies, 5-ALA/PDT has many advantages: 1. lower cytotoxic mechanisms; 2. the ability to easily access the area to be treated through the use of light, especially in the case of tumors that invade hollow organs (by avoiding or reducing normal tissue damage around the treated area); 3. the reduction of long-term morbidity and the possibility to repeat the treatment thanks to a better patient's compliance. Despite such characteristics, it is still considered a palliative therapy and is still investigated its role as a support for canonic therapies. In fact, the use of the light source and the low penetration of light limit the therapeutic applications only to the most superficial areas, or to the most accessible by a light probe. However, the intracellular action mediated by ROS can produce significant effects on the cells with a potentially significant therapeutic aspect. ROS have a lifetime of less than 3,5 μs and can diffuse only 0,01 to 0,02 μm during this period[11]. Due to the limited lifetime, ROS exert their cytotoxic action limited to the site of their localization. When they are concentrate mostly in mitochondria or endoplasmic reticulum (ER), cells die in an apoptotic manner while, if they are concentrate either at the plasma membrane or lysosomes, cells' fate is necrosis or autophagy, respectively[25, 26]. Also the nuclear compartment can be target of ROS even if studies about DNA damage after PDT are still scarcely investigated[27]. It has been reported that photo activation of a HpD caused direct DNA damage[28], as well as production of 8-oxo-Guanine, a typical product of DNA oxidative damage[29].

In all probability, the reason why the nuclear compartment is not targeted by ROS is to be found not only in the limited half-life of the species or in the localization of the PS outside the nucleus but also by other effectors that may contribute to the cause.

1.7 THE ROLE OF ABCG2 IN PHOTODYNAMIC THERAPY

Among the other effectors that may have a role on the effectiveness of PDT, several evidences suggest that ABCG2 (a member of the ATP-binding cassette (ABC) transporters superfamily) is implicated in resistance of cancer cells to PDT.

ABCG2 is located on chromosome 4q22 and was firstly identified as breast cancer resistant protein (BCRP) in doxorubicin-resistant breast cancer cells[30]. It is a so-called "half ABC transporter" due to the fact that is composed by six transmembrane domains and only one ATP-binding cassette (FIGURE 7). In humans, it exist on the plasma membrane as an homodimer and works mainly as exporters of endogenous materials or exogenous drugs from cytoplasm into extracellular environment[31].

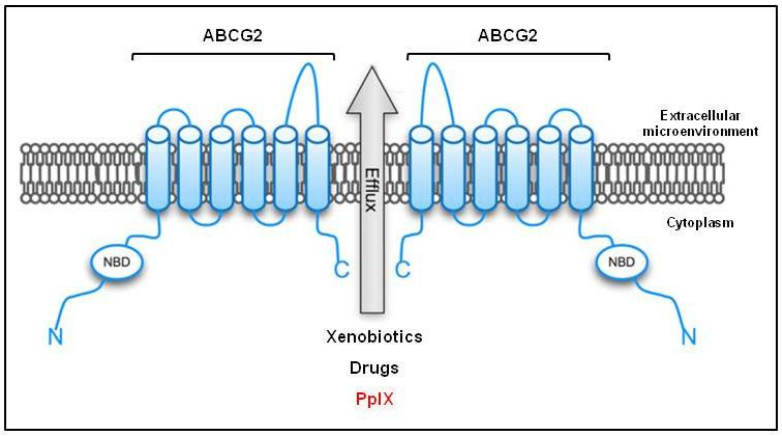

FIGURE 7. Molecular structure of ABCG2 transporter.

ABCG2 is expressed in the plasma membrane of placental trophoblast cells, in the epithelium of the small intestine, in liver canalicular membrane and in ducts and lobules of the breast. In all these compartments, it is involved in a protective role from toxic metabolites or in a regulating role of administered drugs[32]. Several studies indicate that ABCG2 over-expression in transformed cell lines confers resistance to many chemotherapeutic drugs so it is considered one of the main actors in the multi-drug resistance (MDR)[30, 33, 34]. More recently, it was discovered that ABCG2 is able to extrude among its substrates also PpIX so it may have

an important role in the PDT effectiveness[35, 36]. In fact, its over-expression is associated to a reduction of PpIX amount retained within the cells and, consequently, to a reduction of 5-ALA/PDT effectiveness[37, 38].

The expression of ABCG2 is regulated, both in normal and cancer cells, at different levels including epigenetic and transcriptional modifications[31]. It is still unknown at what level the transporter is up-regulated in cells treated with 5-ALA/PDT due to the simultaneous effect of the excess of PpIX inside the cells and the ROS production. Such evidences may throw light on a novel aspect of ABCG2 regulation an may unravel the molecular pathway that subtend its over-expression.

2. AIMS OF THE THESIS

The analysis of DNA damage caused by PDT contributes to a better understanding of the mechanism of oxidation induced DNA damage and may pave the way to improved anti-cancer therapy. Targeted delivery of photosensitizers to the nucleus or long range propagation of ROS-mediated damage are essential tools to potentiate the effectiveness of PDT as tumor-cell killing[39].

To this purpose, the objectives of this study are the following:

a. to explore the biological effects of 5-ALA/PDT on a panel of five cell lines characterized by different levels of p53 and the ATP binding cassette G2 (ABCG2) transporter;

b. to identify the molecular effectors involved in the PDT-induced DNA damage;

c. to unravel the regulation of ABCG2 expression by oxidative stress.

3. MATERIAL AND METHODS

3.1 Cell cultures

Non-small-cell-lung-cancer cell lines H1299 ($p53^{-/-}$) and A549 ($p53^{+/+}$) were obtained from ATCC (Rockville, MD, USA). H1299 cell line was cultured in RPMI 1640 medium, 2 mM L-glutamine, 10 mmol/l HEPES, 1 mM sodium pyruvate, 2.5 g/l glucose, 1.5 g/l sodium bicarbonate, 10% FCS and 1% penicillin/streptomycin; A549 cell line was cultured in F12K medium, 0.75 g/l sodium bicarbonate, 2 mM L-glutamine, 10% FCS and 1% penicillin/streptomycin.

The colorectal HCT-116 colon cancer cells were kindly provided by B. Vogelstein[40] and cultured according ATCC in complete McCoy's 5A medium, consisting of 10% fetal bovine serum, 1% penicillin/streptomycin and 2 mM L-Glutamine. The two lines are $p53^{+/+}$ and $p53^{-/-}$ (the latter obtained by knocking out the p53 gene). The prostatic adenocarcinoma cell line PC3 were obtained from ATCC (Rockville, MD, USA) and cultured in RPMI, 10% FCS, 2 mM L-glutamine and 1% penicillin/streptomycin. Saline solutions, media and serum were all obtained from Gibco (Invitrogen).

3.2 Reagents

5-aminolevulinic acid (Sigma Aldrich) stock solution (300 mM) was dissolved in water, filtered and stored at -20°C. The ABCG2 inhibitor Ko143[41,42] (Sigma Aldrich) stock solution (5 mM) was prepared by solving the powder in DMSO and store at -20°C. H_2O_2 (Sigma Aldrich) was pre-diluted in water (stock solution 1M) before utilized and stored at +4°C. Etoposide (Sigma Aldrich) stock solution (25μg/μl) was dissolved in DMSO and stored at -20°C. The ATM inhibitor KU-55933 (Sigma Aldrich) stock solution (10mM) was prepared by dissolving the powder in DMSO and stored at -20°C.

3.3 PDT treatment

All photodynamic treatments performed throughout this work were carried out on cells as previously described by us and other Authors[43, 44]. All cells were incubated in the dark for 3 h in serum-free medium in the presence of an excess of 5-ALA (0.5 or 1.0 mM), aimed to obtain a greater amount of endogenous PpIX. After incubation, cells were washed 3 times

with Hank's solution (Sigma Aldrich) and then exposed to light. In particular, PDT was administered to cells 72 (H1299 and A549) or 48 hours (HCT-116 ($^{+/+}$ and $^{-/-}$) and PC3) after their seeding. Cells were irradiated using a LED array (S-630, Alpha Strumenti, Melzo, Italy) designed specifically for Photodynamic therapy. The light source was characterized by an emitting wavelength of 630 nm and an irradiance of 5 Jcm^{-2} per minute. The red-light source was placed at a distance from the plates to ensure uniform illumination of the entire cell monolayer. Light fluences used ranged from 0 to 20 Jcm^{-2}. Before further analyses, irradiated cells were released into drug-free complete medium and kept in the incubator as required.

3.4 Protoporphyrin IX measurements

Determination of Protoporphiryn IX production was performed according to Wild et al.[45]. To this purpose ~$1.0x10^5$ H1299 or A549 cells, ~$3.0x10^5$ HCT-116 ($^{+/+}$ and $^{-/-}$) cells and ~$3.5x10^5$ PC3 cells were seeded in 60-mm tissue culture dishes. All steps of these protocols were performed in the dark in order to avoid the photobleaching of Protoporphiryn IX. Cells were incubated without (relative controls) or with ALA (3 hs) in serum-free medium in the dark.

Production of intracellular Protoporphiryn IX was measured in cells after their detaching (by mild trypsinization), washing in PBS, and collection by centrifugation (1200 rpm, 5 min). Cells were resuspended in 1:1 methanol (HPLC grade): perchloric acid (0.9M) and homogenized using an homogenizer (Ultra-Turrax T25-IKA Germany). The suspension was then centrifuged at maximum speed and surnatants quickly transferred into quartz cuvette for fluorescence measurements (emission spectra).

Measurements were performed in Perkin-Elmer spectrofluorimeter setting the excitation wavelength at 406 nm and the excitation and emission slits at 10 nm. Fluorescence spectra were collected between 550 nm and 700 nm.

3.5 Cell Viability Assays

All cells were seeded in 35-mm tissue culture dishes (A549 and H1229, ~5.0×10^4, HCT-116 and PC3, ~1.2×10^5) in triplicate and exposed to PDT as indicated above. The difference in initial cell density is related to the individual different growth rate. In all cases, cell viability was evaluated by Trypan blue assay 24 hours after PDT. No significant changes in cell viability-light fluence dose-response curves were observed when PDT was administered to

cells incubated with 1.0 or 0.5 mM 5-ALA. However, since 1 mM 5-ALA resulted slightly toxic to PC3 cells even in the absence of light, the experiments with PC3 cells, reported therein, have been performed with the lower 5-ALA concentration (0.5 mM).

Routinely, a solution of Trypan blue (Sigma Aldrich, St Louis USA)/trypsinized cell suspensions 1:10 was prepared. Subsequent experiments were performed on the basis of these dose responses curves as only two specific light fluences for each cell line were considered. In particular, we selected the 2 light fluences that induce ~25% or ~50% cell death in each cell line. From the dose response curves the fluences used were 6 and 12 Jcm^{-2} for H1299, 4 and 8 Jcm^{-2} for A549, 7.5 and 15 Jcm^{-2} for HCT-116 $^{+/+}$, 10 and 20 Jcm^{-2} for HCT-116 $^{-/-}$, 5 and 10 Jcm^{-2} for PC3 cells, respectively. This kind of selection allowed us to consider the different cells in conditions that determine, independently from the cell line used, the same reduction of viability. Residual viability was expressed as percentage (mean ± SD) of trypan blue–negative cells versus untreated controls.

3.6 Cell cycle analysis

Cells (~1.0×10^5 H1299 and A549, ~3.0×10^5 HCT-116, and ~3.5×10^5 PC3) were seeded in 60-mm tissue culture dishes in triplicate and exposed to PDT as detailed in the section 3.3. As stated before, only two fluences were chosen for each cell line, namely 6 and 12 Jcm^{-2} for H1299, 4 and 8 Jcm^{-2} for A549 cells, 10 and 20 Jcm^{-2} for HCT-116 $^{-/-}$, 7.5 and 15 Jcm^{-2} for HCT-116 $^{+/+}$, 5 and 10 Jcm^{-2} for PC3 cells. Six hours after PDT, cells were detached by trypsinization, washed in PBS, and fixed in 70% ethanol. Before analysis, cells were washed in PBS, resuspended in a PBS solution containing RNase (Roche) and propidium iodide (Sigma Aldrich), and stored in the dark for 20 min at RT. Fluorescence was detected using the 488 nm laser line with a CyAn ADP Flow Cytometer (DAKO Cytomation, Milan, Italy). Not less than 20000 events (≥ 15000 cells) were recorded for each sample. Cell cycle profiles were analyzed using ModFit/LT 3.2 version (Verity Software, Topsham, ME, USA). Data were obtained from three independent experiments (triplicate samples) and expressed as mean ± SD.

3.7 Alkaline Comet assays

Cells were dealt exactly as for cell-cycle analysis (see above). Six hours after PDT, were detached by trypsinization, washed once with PBS, centrifuged and resuspended in PBS (1.0 x 10^5 cells/ml). Alkaline comet assay was performed according to the instructions provided by the kit manufacturer (Trevigen, Helgerman, CT, USA). Cells were combined with molten low melting Agarose (at 37°C) and pipetted onto CometSlide™. Slides were incubated at 4°C for 20 min in the dark for the agarose to gel and the sample became adherent to the slide. Slides were then immersed in pre-chilled lysis solution for 45 min and subsequently in alkaline unwinding solution for 45 min in the dark. Slides were transferred in a horizontal electrophoresis apparatus (30 min, 1 V/cm, 300 mA), covered with alkaline electrophoresis solution, washed twice with H_2O, incubated in ethanol for 5 min, air dried, stained with SYBR™ Green and analyzed by fluorescence microscopy. For each sample more than 100 cells were collected. Only undamaged DNA retains round shape, while damaged DNA migrates away from the nucleus, depending on the molecular weight of its fragments, acquiring the characteristic comet shape. Cell images were analyzed using COMET Score™ (TriTek, Annandale, VA, USA) to quantify DNA damage through measurements of the Comet tail moment, Olive moment and % DNA tail[46]. The fluorescence (arbitrary units) of tail moment, olive moment and % DNA tail has been reported as function of applied light fluences (mean ± SD).

3.8 Histone H2AX phosphorylation assays

Cells, dealt with as for cell-cycle analysis (see above), were washed (3 times) with a colorless Hank's solution (Sigma Aldrich, St Louis USA), irradiated and released in fresh complete culture medium for 6h, detached with trypsin, centrifuged, washed with PBS (twice), and re-suspended in 70% ethanol. To detect γ-H2AX, cells were incubated with anti-γ-H2AX (ser139) monoclonal antibody (Upstate) in 4% FBS TBS-T 0.1% for 2h at RT. Cells were washed with TBS-T 0,1% and incubated with a fluorescein-tagged anti-mouse secondary antibody (Sigma Aldrich, St Louis USA) in 4% FBS TBS-T 0.1% for 1h at RT in the dark. After washing with TBS-T 0.1%, cells were resuspended in TBS then analyzed in a CyAn ADP Flow Cytometer (DAKOCytomation) equipped with an excitation laser line at 488 nm. The data collected were analyzed using the Dako Summit Software version 4.3. The observed shift of the fluorescence signal (referred to the curve mean) was referred to the position in the

untreated control and expressed as percent (mean ± SD). About 20000 events (i.e., fluorescence readings, corresponding to not less than 15,000 cells) were recorded for each sample (triplicates).

3.9 ABCG2 inhibition

To induce ABCG2 protein inhibition, A549 and PC3 cells were treated with 1.5 and 2.0 μM Ko143 respectively[30]. The inhibitor has been added to the culture medium together with ALA in serum-free medium and then is re-added in the complete culture medium after light irradiation, until cells are harvested and analyzed. Although Ko143 has been considered a specific inhibitor of ABCG2, at high concentrations[42] it inhibits also ABCB1 and ABCC1. In this work Ko143 concentration used was ≤ 2.0 μM[42, 47] . Under these conditions (detailed in the respective figure legends), Ko143 inhibits specifically ABCG2.

3.10 PpIX intracellular localization

H1299 (1.0 x 10^5) and PC3 (3.5 x 10^5) cells were grown onto glass coverslips, allowed to adhere, then exposed to PDT; fluences used were 6 and 10 Jcm^{-2} for H1299 and PC3 cells, respectively. After irradiation the cells were washed with PBS, fixed and analyzed at time 0 h, or released in fresh culture medium and analyzed 6 h later. Cells treated with 5-ALA and did not irradiate (controls) were processed and analyzed at the same times of the irradiated ones.
Cells were fixed in PBS/4% formaldehyde for 10 min in the dark. After further washes with PBS, samples were mounted and viewed with an LSM 710 inverted confocal laser-scanning microscope (Zeiss).

3.11 Western blot analysis

ABCG2 detection after PDT: Appropriate quantities of protein extracts were obtained from the following cell numbers: ~1.0 x 10^5 H1299 or A549; ~3.0 x 10^5 HCT-116 or PC3; exposed to the following fluences: 6 and 12 Jcm^{-2} for H1299; 4 and 8 Jcm^{-2} for A549; 10 and 20 Jcm^{-2} for HCT-116 $^{-/-}$; 7.5 and 15 Jcm^{-2} for HCT-116 $^{+/+}$; and 5 and 10 Jcm^{-2} for PC3 cells.
Cells were harvested 0.5, 1, 3 and 6 hours after PDT. Cellular pellets were suspended in lysis buffer; the proteins extracted were measured as previously reported[48, 49]. Polyacrylamide gels (stacking gel: 4% acrylamide, running gel:10% acrylamide) were prepared as described by

Laemmli[50]. Proteins separated on polyacrylamide gels were blotted onto nitrocellulose filters (Perkin Elmer). Molecular weight standards were from Fermentas Life Sciences (M-Medical, Milan, Italy). Filters were washed in PBS-T 0.1%, soaked in 5% non-fat dry milk in PBS-T 0.1%, incubated with specific primary antibodies and then with secondary antibodies (Santa Cruz) conjugated to horseradish peroxidase (BioRad). The primary antibody against ABCG2 was from Santa Cruz (CA, USA); anti-tubulin was provided by ABM (Richmond BC, Canada). Finally filters were developed using an electro-chemiluminescent western blotting detection reagent (Roche).

ABCG2 detection on PC3 after treatment with H_2O_2 or Etoposide: Appropriate quantities of protein extracts were obtained from ~3.5 x 10^5 PC3 cells. After 48 hours, cells were incubated with 1 mM H_2O_2 and then harvested 0.5, 1 and 3 hours later or 25 ng/μl of Etoposide in serum-free medium and then harvested 0.5, 1 and 4 hours later. Cellular pellets were treated and analyzed as reported above.

3.12 RNA extraction, cDNA synthesis and RT-PCR

For mRNA expression, ~3.5 x 10^5 PC3 cells were seeded in 60-mm tissue culture dishes and then treated after 48 hours. For single treatment with Etoposide, cells were treated as indicated above. For combined treatment with KU-55933, cells were first pre-treated with 10 μM in serum-free medium with the ATM inhibitor and then treated with Etoposide as above. Total RNA was extracted using Trizol (Gibco, Invitrogen) 0.5, 1 and 4 hours later for single treatment or 0.5 and 1 hour later last treatment for the combined one. Samples were quantized with NanoDrop 2000c (Thermo Fisher Scientific, Life technologies). RNA (1μg) was reverse transcribed (RT) using a high-capacity reverse transcriptase kit (SensFAST cDNA Synthesis Kit, Bioline) according to manufacturer's instructions. The mRNA level (50 ng for each cDNA) of ABCG2 was measured by on a StepOnePlus on DNA template (RT-PCR) System (Applied Biosystems) using the SYBR Green-detection system (Biorad) according to manufacturer's instructions. Following primers were used for ABCG2 cDNA amplification: (ABCG2 FW) 5'-AGC AGC AGG TCA GAG TGT GGT-3' and (ABCG2 RV) 5'-TGC ATT GAG TCC TGG GCA GAA GT-3'. The levels of the housekeeping 18S transcript were used as a control for equal cDNA loading: (18S FW) 5'-GCG CTA CAC TGA CTG GCT C-3' and (18S RV) 5'-CAT CCA ATC GGT AGT AGC GAC-3'. The thermal protocol was: 95° for 5 sec, 95° for 15 sec, 55° for 20 sec, 72° for 30 sec (40 cycles), 95° for 5 sec, 65° for 1 min

(melting curves); reaction was stopped at 4°C. Calculations of relative expression levels were performed using the $2^{-\Delta\Delta Ct}$ method[51] and take into account the values of at least two independent experiments performed in triplicate.

3.13 Statistical analysis

Significance was assessed using unpaired Student's t test for comparison between two means (P values: *<0.05; **<0.01; ***<0.001).

4. RESULTS

4.1 5-ALA/PDT AFFECTS CELL VIABILITY.

To evaluate whether p53 had a role in protecting cells from the effect of photodynamic therapy we analyzed cell lines expressing p53 (A549 and HCT-116$^{+/+}$) and cells constitutively p53 null or knock out derivatives (H1299, PC3 and HCT-116$^{-/-}$ respectively). All cell lines analyzed are able to uptake exogenous 5-ALA, independently of the status of p53. 5-ALA is metabolically converted into the photosensitizer PpIX, as indicated by the characteristic shape of fluorescence spectra peaking at 604 nm and 670 nm (FIGURE 8).

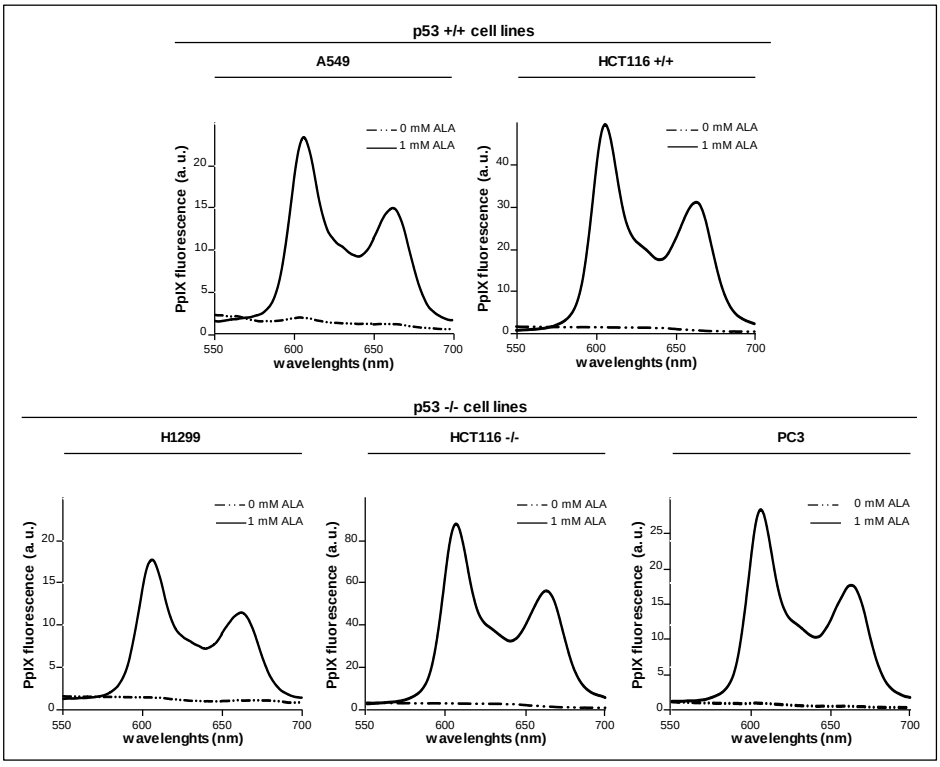

FIGURE 8. Fluorescence emission spectra of PpIX in the five cell lines analyzed.

Cells viability was assessed by Trypan blue assay. Cells were incubated with 5-ALA for 3 hours and then irradiated with increasing doses of light. The assay has been performed 24 hours after the release into drug-free complete medium (FIGURE 9).

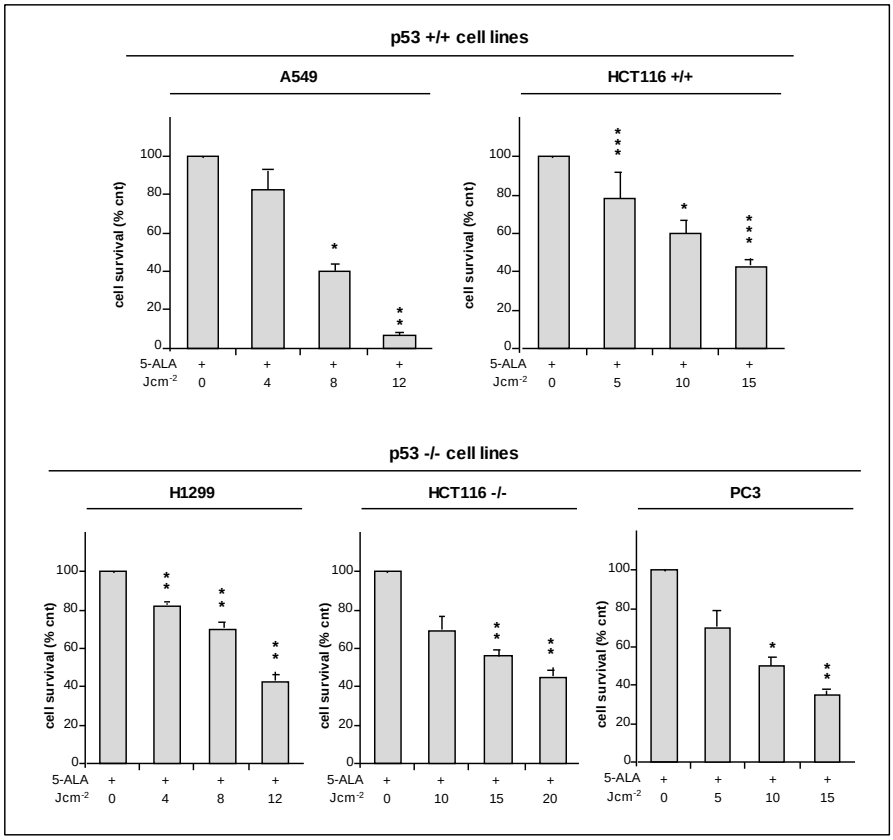

FIGURE 9. **Residual cell viability assessed by Trypan blue assay.** Cells viability of A549, HCT-116$^{+/+}$, H1299, HCT-116$^{-/-}$ and PC3 are expressed as percentage of untreated controls in function of light fluence. Each bar is the average of triplicate measurements (mean±SD). Statistical significance (relative to control): $^{*}P < 0.05$; $^{**}P < 0.01$; $^{***}P < 0.001$.

5-ALA/PDT affects cellular viability in all cell lines tested in a light-dose dependent manner. PDT response is remarkably similar in all cell lines, regardless of p53 expression. In order to compare the different cell lines, subsequent experiments were performed using only two light fluences for each cell line which induce ~25% or ~50% cell death. Chosen fluences were: 6 and 12 Jcm^{-2} for H1299, 4 and 8 Jcm^{-2} for A549, 7.5 and 15 Jcm^{-2} for HCT-116$^{+/+}$, 10 and 20 Jcm^{-2} for HCT-116$^{-/-}$, 5 and 10 Jcm^{-2} for PC3 cells.

4.2 5-ALA/PDT CAUSES CELL CYCLE ALTERATIONS

To evaluate whether 5-ALA/PDT has a potential effect on cell cycle profiles, we performed a cytofluorimetric analysis. All cell lines were irradiated using the conditions already discussed and cell cycle profiles were collected 6 hours after PDT.

A549 ($p53^{+/+}$) and PC3 ($p53^{-/-}$) do not present significant alterations of the cell cycle profiles, which are very similar to the respective controls (FIGURE 10).

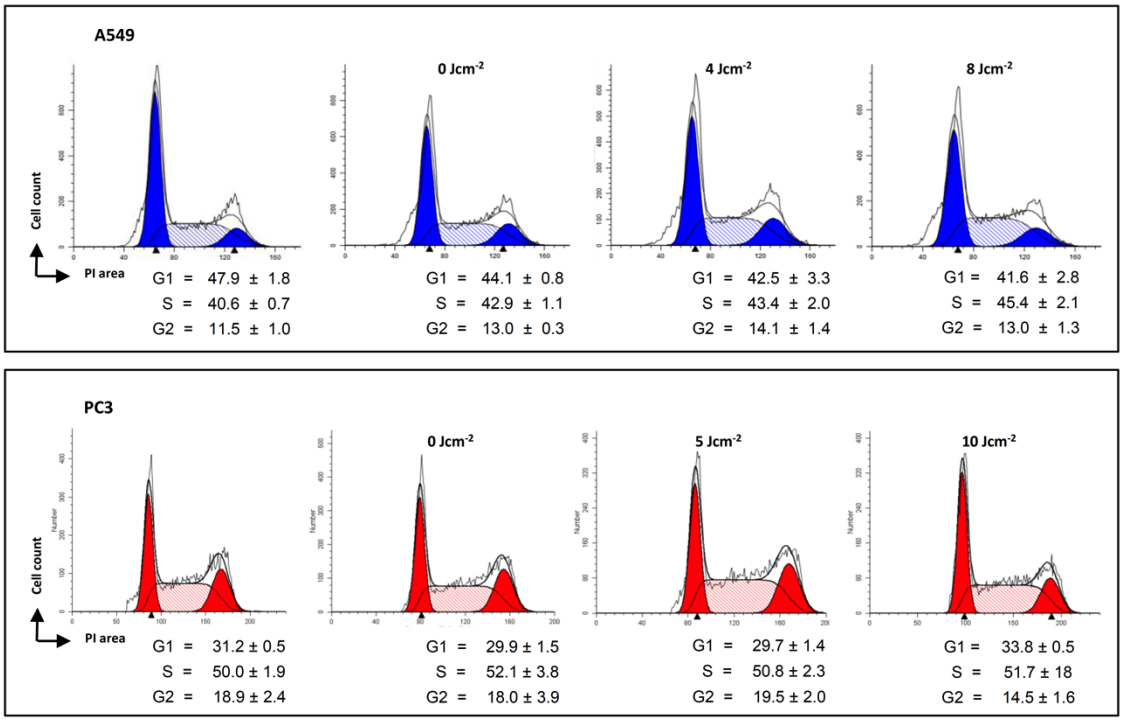

FIGURE 10. C**ell cycle profiles of A549 and PC3 cell lines.** Cytofluorimetric assay were performed 6 hours after PDT in A549 and PC3 cell lines. The figure reported representative cell cycle profiles. Numerical data of the phase cycle reported under the various panels are the average of triplicate measurements (mean±SD). Statistical significance (relative to control): $^{*}P < 0.05$; $^{**}P < 0.01$; $^{***}P < 0.001$.

By contrast, the other cell lines (H1299 and both clones of HCT-116) display significant alterations of the cell cycle (FIGURE 11).

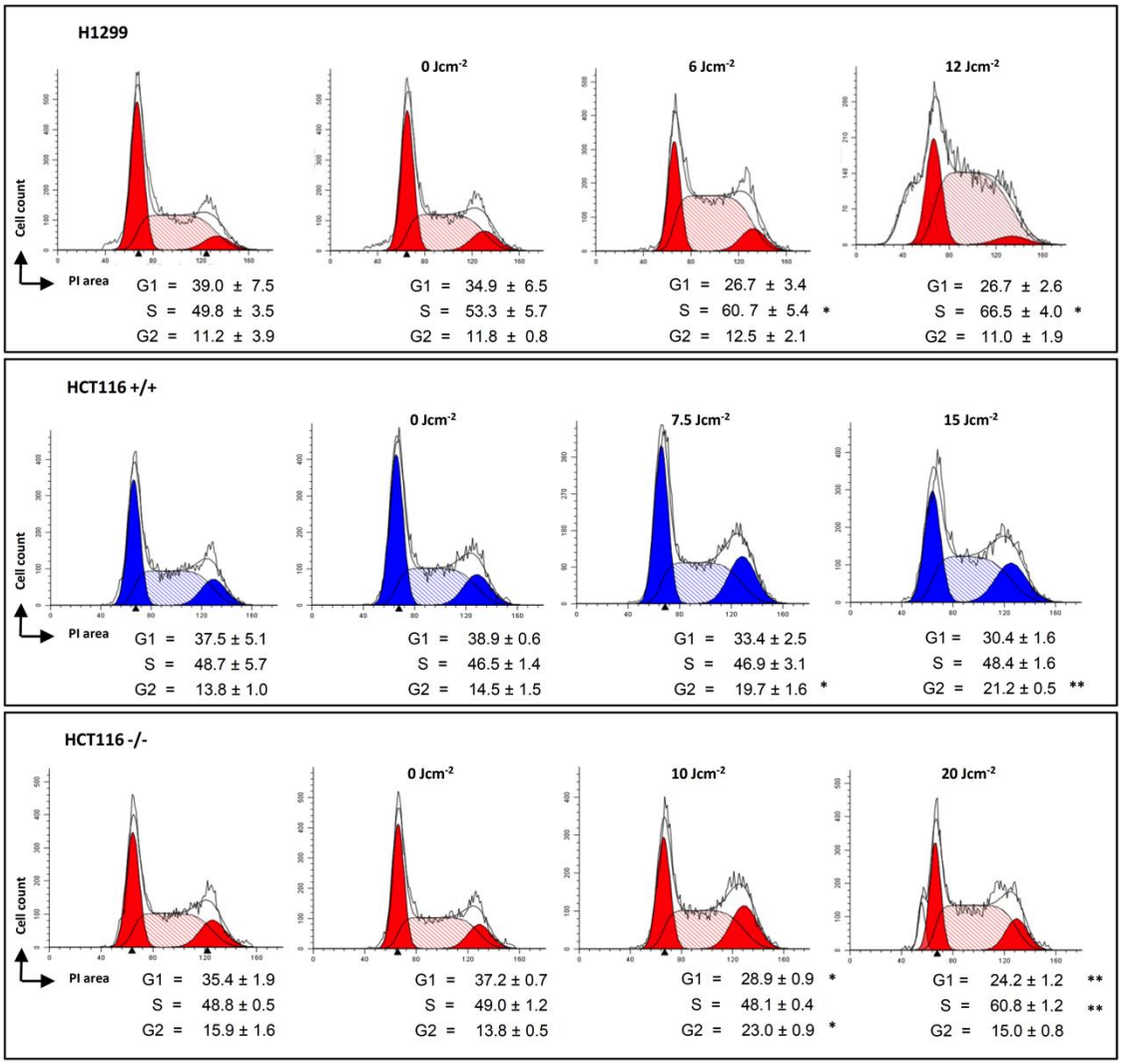

FIGURE 11. C**ell cycle profiles of H1299 and HCT-116 (both clones).** Cytofluorimetric assay were performed 6 hours after PDT in H1299, HCT-116$^{+/+}$ and HCT-116$^{-/-}$ cell lines. The figure reported representative cell cycle profiles. Numerical data of the phase cycle reported under the various panels are the average of triplicate measurements (mean±SD). Statistical significance (relative to control): *P <0.05; **P <0.01; ***P <0.001.

In H1299 cells 5-ALA/PDT determines a significant arrest of cells in S phase, which increases with the dose of light applied (FIGURE 11, upper panel).

On the other hand, also HCT-116$^{+/+}$ cells display cell cycle alterations. Cell cycle arrest interests the G_2 phase and it is also dependent on the dose of light applied (FIGURE 11, middle panel).

Equally significant cell population shifts occur in HCT-116$^{-/-}$: at the lower dose of light these cells arrest essentially in G_2 phase while, at higher light doses the cells arrest in S phase (FIGURE 11, lower panel**).**

PpIX and consequently ROS propagation reached the nuclear compartment in H1299 and HCT116 cell lines. A549 and PC3 did not show significant cell cycle alterations. These data suggest that 5-ALA/PDT can cause DNA damage in sensitive cell lines.

4.3 CELL CYCLE ALTERATIONS CORRELATE WITH γ-H2AX HISTONE PHOSPHORYLATION

To test the hypothesis that 5-ALA/PDT induces DNA damage in sensitive cell lines, we performed cytofluorimetric analysis to evaluate the PDT-induced accumulation of phosphorylated γ-H2AX histone. Phospho-γ-H2AX is phosphorylated by the checkpoint kinase ATM and marks double strand DNA breaks).[52, 53]

Cells were treated and irradiated as indicated above and successively analyzed (6 hours after irradiation) to measure the levels of γ-H2AX phosphorylation on Ser139 (FIGURE 12).

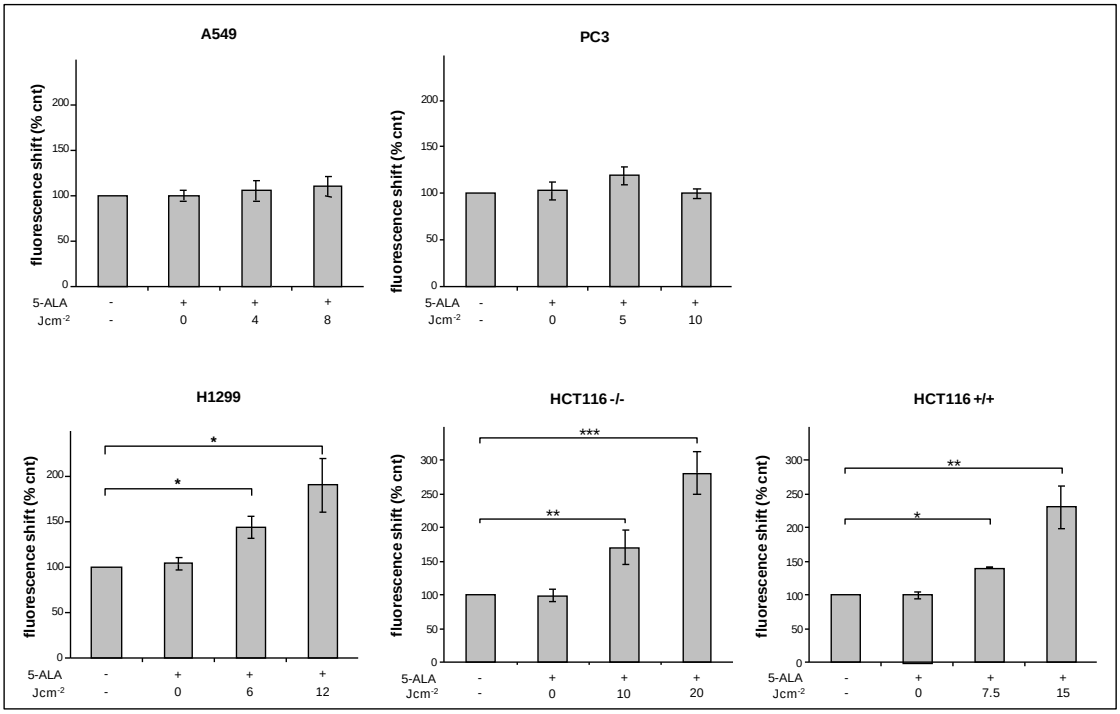

FIGURE 12. γ-H2AX phosphorilation status after 5-ALA/PDT. Cytofluorimetric evaluation of γ-H2AX phosphorilation on Ser139 6 hours after PDT. Cells were grouped on the bases of the presence/absence of significant fluorescent shift. Phosphorylation levels are expressed as percentage of untreated controls. Each bar is the average of triplicate measurements (mean±SD). Statistical significance (relative to control): $^{*}P < 0.05$; $^{**}P < 0.01$; $^{***}P < 0.001$.

Phospho- γ-H2AX accumulates upon PDT in the DNA of same cell lines that present cell cycle alterations (FIGURE 12). A549 and PC3 do not show any accumulation of phospho γ-H2AX at any dose of light. Accumulation of phospho-γ-H2AX is in all cases light–dependent. On the other hand, treatment with 5-ALA by itself does not induce γ-H2AX histone activation.

p53 status is not associated with light-induced DNA damage. In fact, both HCT116 lines ($p53^{+/+}$ and $p53^{-/-}$) and PC3 ($p53^{-/-}$) cell lines showed slight fluence-dependent phospho-γ-H2AX phosphorylation levels. Thus, p53 does not appear to be sufficient to protect nuclear DNA damage from PDT.

4.4 5-ALA/PDT INDUCES DNA DAMAGE IN H1299 AND HCT-116 CELL LINES

To strengthen the evidence of DNA damage in cell lines exposed to PDT, we decided to perform a Single Cell Gel Electrophoresis, otherwise known as "Comet Assay" because is considered a pivotal method to assess DNA damage. This assay exploits the property of DNA to maintain its integrity during an electrophoresis migration if it is not perturbed. Conversely, breaks in its structure make it free to migrate. DNA fragments assume the shape of the "tails" of the rounded "heads"; hence the formation of a "comet". The extent of DNA breaks reflect the proportion of DNA that moves into the tail. Comet Assay is analyzed by three parameters: "tail moment", "% DNA tail mean", and "olive moment mean". The "tail moment" is a parameter that takes into account DNA migration and the relative amount of DNA in the tail. The "% of DNA tail" quantifies the ratio between the fluorescence intensity of the head and tail (in a range from 0 to 100%). The "olive tail moment" is an index generated by the product of the tail length multiplied the % tail DNA.[46]

Alkaline Comet Assay was performed under the same experimental conditions indicated above. Irradiated H1299 and HCT-116 cells display the comets and comet length's tail increases with the light dose (FIGURE 13) as indicated also by the increase of the DNA tail, tail moment and olive moment.

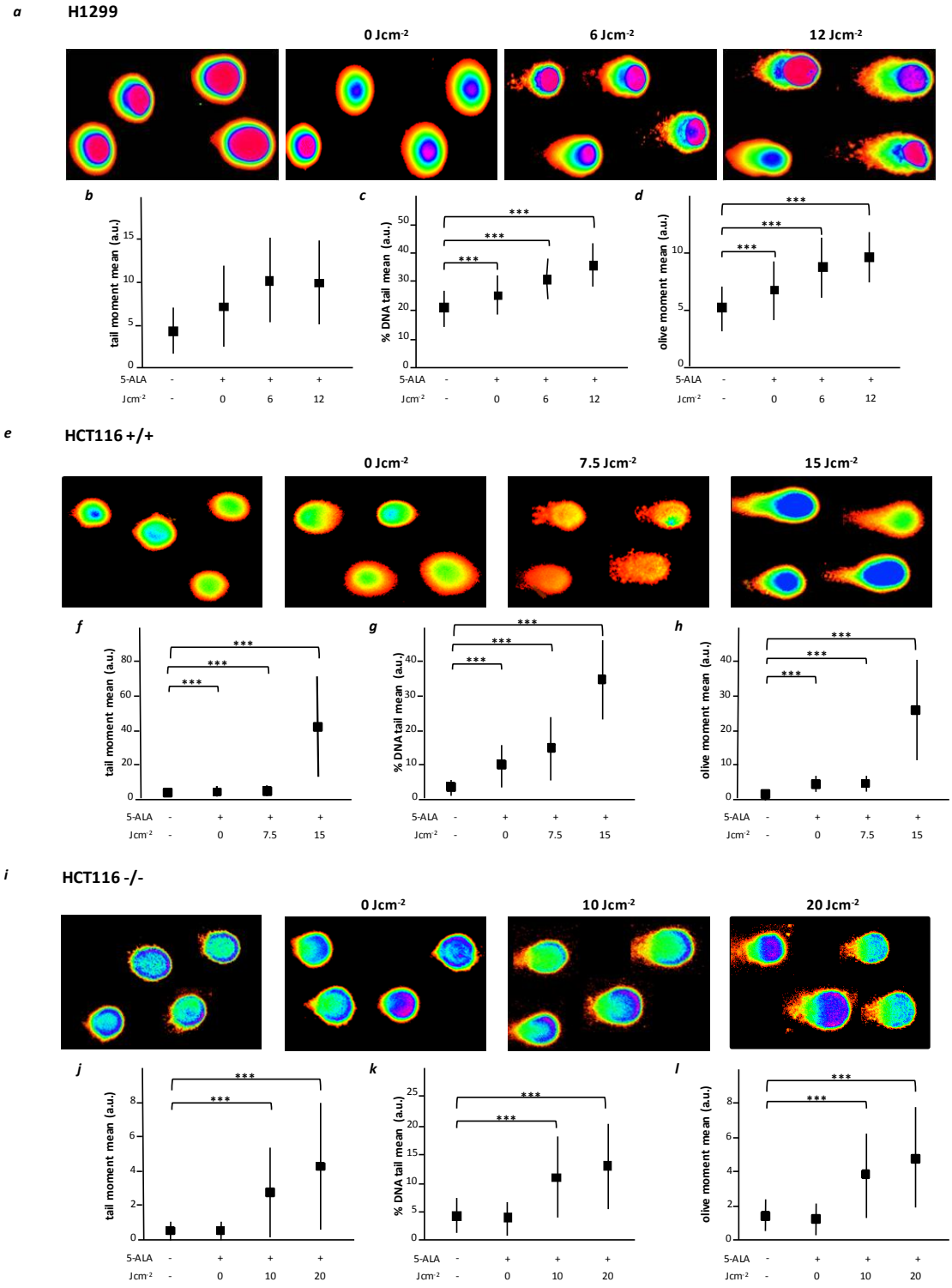

FIGURE 13. Comet Assay for H1299, HCT-116$^{+/+}$ and HCT-116$^{-/-}$ cell lines. Comets images collected at 6 hs after PDT treatment through COMET ScoreTM software (TriTek Corp.) for H1299, HCT-116$^{+/+}$ and HCT-116$^{-/-}$ cells (panels a, e and i, respectively). Tail moment mean (a. u.) as function of light fluence (panels b, f, j, respectively). for H1299, HCT-116$^{+/+}$ and HCT-116$^{-/-}$ cells. Percentage of DNA tail (a. u.) as function of light fluence for H1299, HCT-116$^{+/+}$ and HCT-116$^{-/-}$cells (panels c, g and k, respectively). Olive moment (a. u.) as function of light fluence for H1299, HCT-116$^{+/+}$ and HCT-116$^{-/-}$cells (panels d, h and l, respectively). Each point represents the fluorescence of > 100 cells (mean ± SD). Statistical significance (in respect to control) P values: * < 0.05, ** < 0.01, *** < 0.001.

The comet assay performed in A549 and PC3 cells did not show any significant alteration (FIGURE 14). Irradiated cells maintain their rounded shape if compared to the controls, without any appreciable variation of the parameters analyzed.

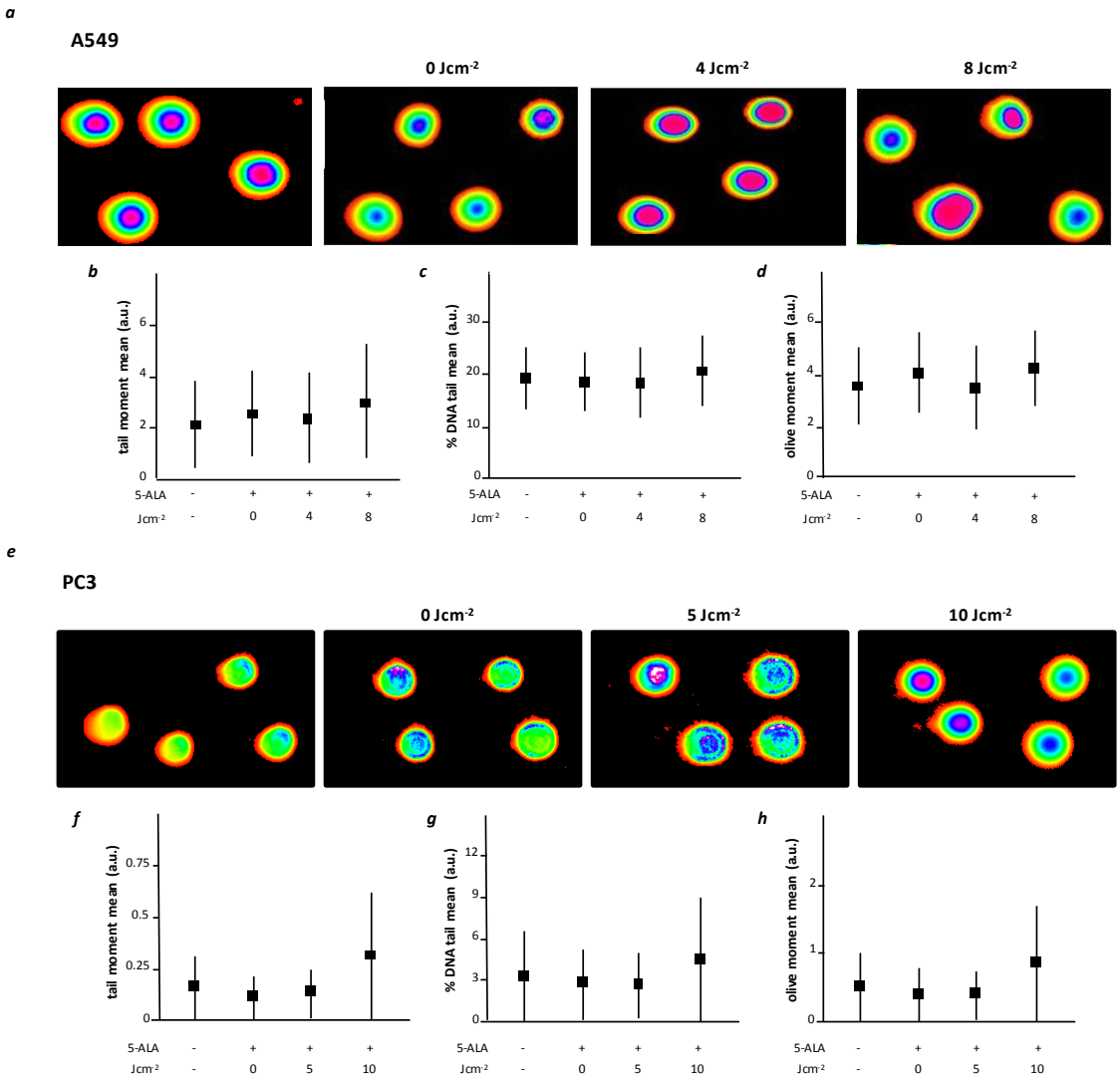

FIGURE 14. **Comet Assay for A549 and PC3 cell lines**. Comet images collected at 6 hs after PDT treatment through COMET ScoreTM software (TriTek Corp.) for A549 and PC3 cells (panels a and e, respectively). Tail moment (a. u.) as function of light fluence for A549 and PC3 cells (panels b and f, respectively). Percentage of DNA tail (a. u.) as function of light fluence for A549 and PC3 cells (panels c and g, respectively). Olive moment (a. u.) as function of light fluence for A549 and PC3 cells (panels d and h, respectively). Each point represents the fluorescence of > 100 cells (mean ± SD). Statistical significance (in respect to control) P values: * < 0.05, ** < 0.01, *** < 0.001.

4.5 DNA DAMAGE INVERSELY CORRELATES WITH THE LEVELS OF ABCG2 TRANSPORTER

It is known that ABCG2 (the ATP-binding cassette (ABC) transporter G2) has a role in regulating cellular accumulation of PpIX (and, more in general, porphyrin derivatives) in several cancer cells[32]. Hence, its ability to extrude PpIX could affect the response of cells to PDT.

We analyzed the expression of ABCG2 in all cell lines before and after 5-ALA/PDT at different times. As reported in FIGURE 15, the five cells lines present different levels of the transporter and they can be sub-divided into lower and higher ABCG2 producers.

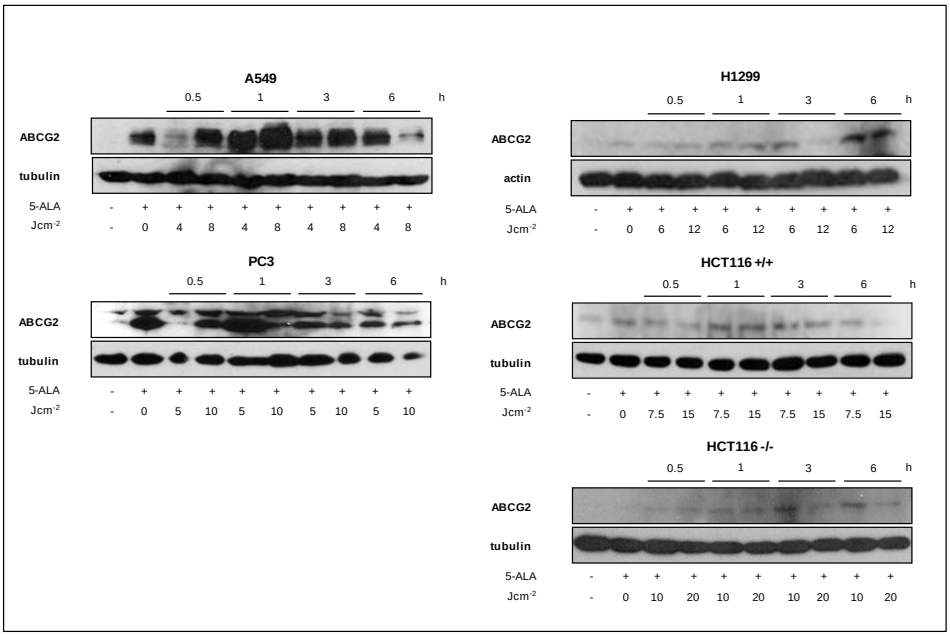

FIGURE 15. **Expression profile of ABCG2**. All cell lines have been schematized according to the presence/absence of ABCG2. Western Blot analyses were performed at 0.5, 1, 3 and 6 hs after PDT treatment. Tubulin was used as loading control.

H1299 and HCT-116 contain low levels of ABCG2 protein (FIGURE 15, right panels) and accumulate DNA damage after light exposure. Conversely, A549 and PC3 contain high levels of ABCG2, which oscillate during the period of time after treatment (FIGURE 15, left panels) and present low levels of DNA damage [47, 54, 55].

γ-H2AX histone activation (FIGURE 12) and Comet assay (FIGURE 13 AND 14) suggest that there is an inverse relationship between ABCG2 transporter levels and DNA damage PDT mediated. In fact, A549 and PC3, containing high levels of the transporter are resistant to

PDT-induced DNA damage. On the other hand, H1299 and HCT116 containing low ABCG2 levels accumulate a significant DNA damage after PDT.

4.6 PPIX REACHES NUCLEAR COMPARTMENT IN THE ABSENCE OF ABCG2.

To induce DNA damage, PpIX must localize nearby the nucleus during irradiation to propagate ROS and oxidation products immediately after irradiation to the DNA. We have hypothesized that, in the absence of ABCG2, PpIX reaches the perinuclear area and mediates light-dependent damage. When ABCG2 is present, PpIX is extruded rapidly and DNA cannot be damaged by photoactivation.

To validate this hypothesis, we decided to visualize the localization of PpIX in cells treated with 5-ALA by exploiting the spontaneous fluorescence of PpIX. Confocal microscopy analysis was performed in H1299 ($p53^{-/-}$; low ABCG2) and PC3 ($p53^{-/-}$; high ABCG2) to measure intracellular PS (FIGURE 16).

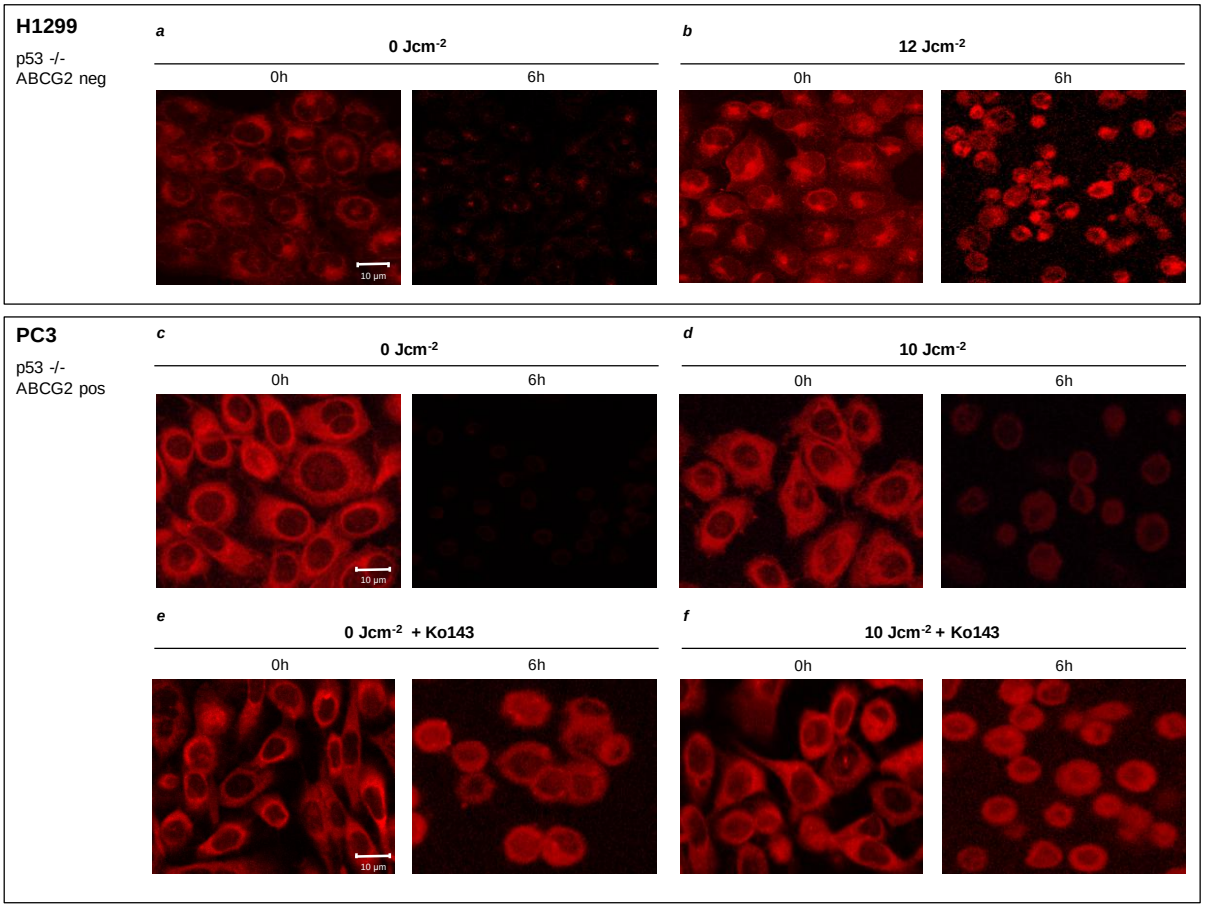

FIGURE 16. **PpIX distribution in H1299 and PC3 cell lines, with and without Ko143.** Confocal microscopy of H1299 cells (panels *a* and *b*) and PC3 cells (panels *c*-*f*) after incubation with 5-ALA and, where indicated, 6 hours after irradiation. PpIX is revealed by the red fluorescence (more details in the text).

Both cell lines were irradiated at the highest light dose (6 and 10 Jcm^{-2}, respectively) and analyzed immediately after incubation with 5-ALA or 6 hours later after PDT.

After incubation with 5-ALA, H1299 shows PpIX mostly localized in the cytoplasm and in the perinuclear area, while, 6 hours later, the fluorescence slowly disappeared (FIGURE 16, panel *a*). Immediately after irradiation, PpIX localization is not altered. Conversely, 6 hours after irradiation (concomitant with DNA damage) PpIX fluorescence is detected in the nuclear area (FIGURE 16, panel *b*). Also in PC3 cells PpIX localizes in the cytoplasm and in the perinuclear region after 5-ALA incubation and, similarly to H1299, 6 hours later the fluorescence signal disappears (FIGURE 16, panel *c*). PC3 cells differ significantly from H1299 6 hours after irradiation. In fact, at this time, PpIX fluorescence is not detectable (FIGURE 16, panel *d*) and DNA damage is not present. One important difference between the two cell lines is the presence of significant levels of ABCG2. To demonstrate a direct involvement of ABCG2 in DNA damage after PDT, we used an ATP-binding cassette inhibitor namely Ko143 which, at concentrations below 1 µM, selectively inhibits ABCG2.[42]

Incubation of the cells with Ko143 maintains the PpIX fluorescence signal inside the cells after incubation with 5-ALA up to six hours (FIGURE 16, panel *e*). Moreover, after PDT in inhibitor-treated cells, PpIX fluorescence labels the perinuclear area (FIGURE 16, panel *f*). These data indicate that inhibition of ABCG2 results in cytoplasmic and, eventually, nuclear localization of PpIX. As an indirect sign of DNA damage, six hours after PDT, the cells change morphology and acquire a rounded shape, which is a sign of stress. Conversely, in control cells (not treated with Ko143) the fluorescence signal rapidly disappears resulting in resistance to light-induced DNA damage. As expected, in cells expressing very low levels of ABCG2, such as H1299, Ko143 did not modify PpIX fluorescence (data not shown).

4.7 DNA DAMAGE OCCURS IN ABCG2 POSITIVE CELL LINES IN PRESENCE OF THE INHIBITOR KO143

The above experiments indicate that the localization of PpIX in the perinuclear area is essential for DNA damage induced by PDT. Inhibition of ABCG2 prevents PpIX extrusion from the cells causing more efficiency cell death by PDT, due to high levels of PS that can re-localized in the nuclear compartment. Under these conditions, PDT-resistant cells should become sensitive to light induced cell death. To demonstrate that ABCG2 is involved in PDT cell death resistance, we performed a Comet Assay in A549 and PC3 cells in the presence of Ko143 (FIGURE 17).

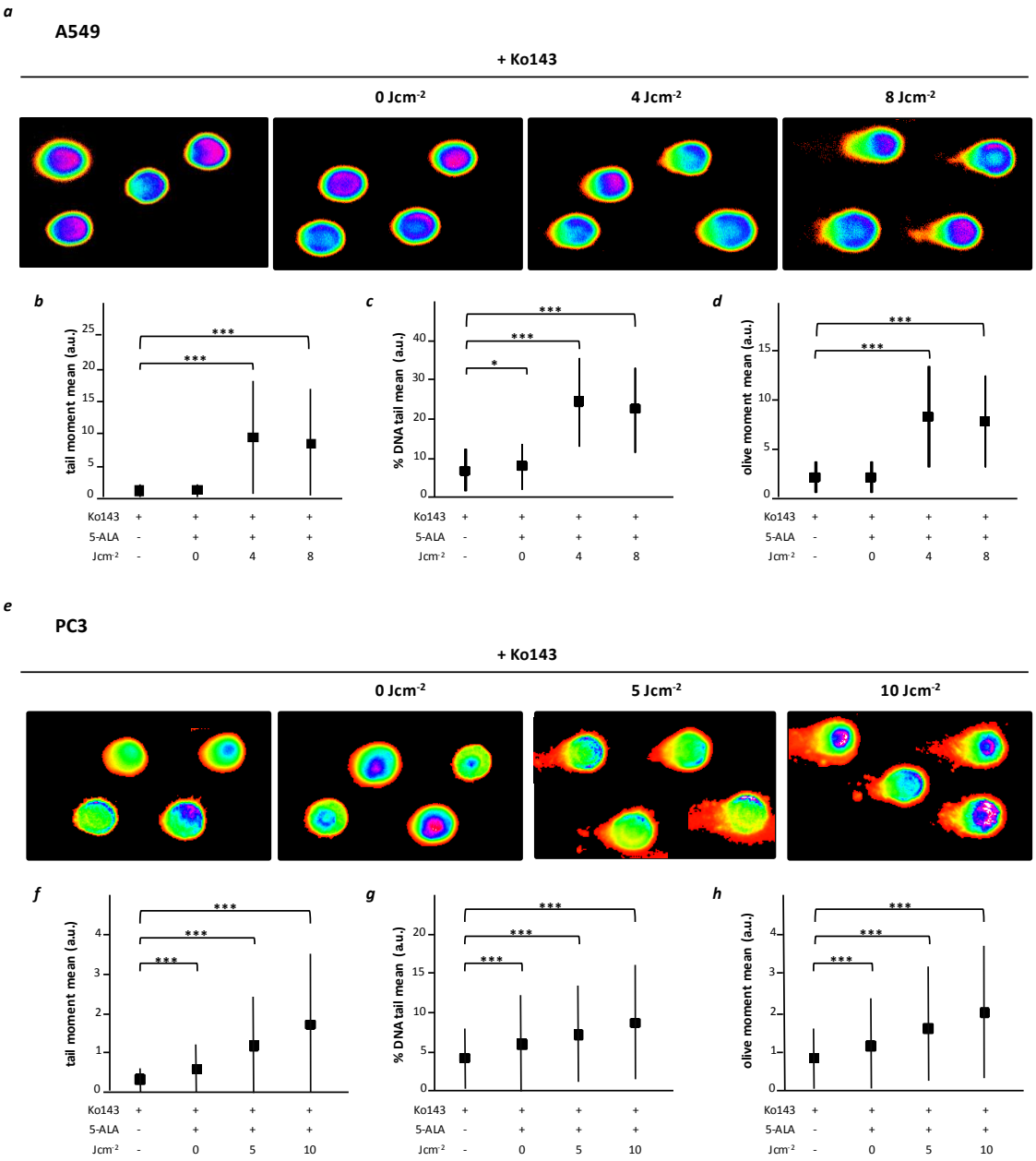

FIGURE 17. **Comet assay for A549 and PC3 cells after treatment with Ko143.** Comets images collected at 6 hs after PDT treatment in the presence of Ko143 through COMET ScoreTM software (TriTek Corp.) for A549 and PC3 cells (panels a and e, respectively). Tail moment (a. u.) as function of light fluence for A549 and PC3 cells (panels b and f, respectively). Percentage of DNA tail (a. u.) as function of light fluence for A549 and PC3 cells (panels c and g, respectively). Olive moment (a. u.) as function of light fluence for A549 and PC3 cells (panels d and h, respectively). Each point represents the fluorescence of > 100 cells (mean ± SD). Statistical significance (in respect to control) P values: * < 0.05, ** < 0.01, *** < 0.001.

A549 and PC3 cells show a significant increase of the number and size of comets when exposed to PDT. Moreover, under these conditions there was a significant increase of tail moment, of % DNA tail and of olive moment (FIGURE 17, panels *b-d* and *f-h*).
These data indicate that ABCG2 activity mediates the resistance to DNA damage PDT-mediated.

4.8 DNA DAMAGE INDUCES ABCG2

Our data indicate that ABCG2 transporter levels increase after stress (5-ALA/PDT) but it is still unknown whether its expression depends on the ROS generated after irradiation or on the increased levels of PpIX *per se*.
To unravel the mechanism(s) underlying ABCG2 induction, we first investigate whether ABCG2 levels are induced by ROS produced by H_2O_2[56]. To this end, we selected PC3 cell lines ($p53^{-/-}$) to eliminate the contribution of p53 in stress-response regulation (FIGURE 18).

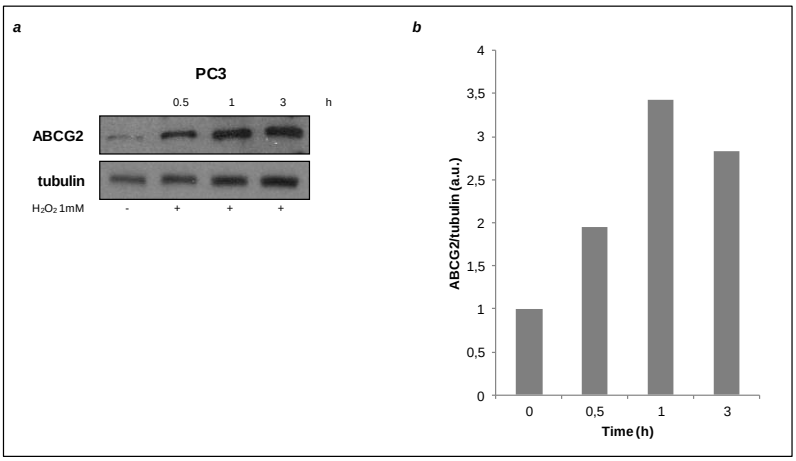

FIGURE 18. **ABCG2 expression in PC3 after treatment with H_2O_2.** Panel *a*: Western Blot analyses were performed at 0.5, 1 and 3 hs after H_2O_2 treatment. Tubulin was used as loading control. Panel *b*: Relative densitometry of the Western Blot.

ROS produced stimulate ABCG2 protein levels and replicate the timing of the induction by PDT. We next tested whether DNA damage may affect ABCG2 expression levels. To this end we measured ABCG2 levels in cells exposed to Etoposide, a selective inhibitor of topoisomerase II enzyme that is able to induce DNA damage[57] (FIGURE 19).

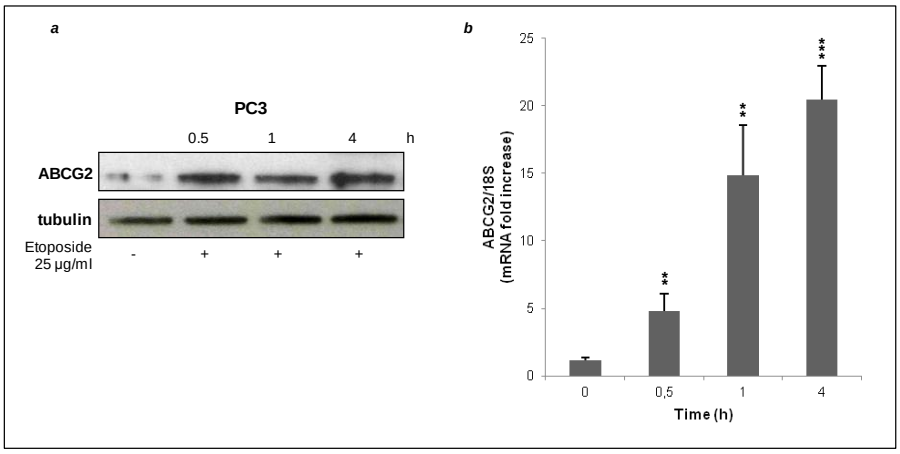

FIGURE 19. **ABCG2 expression levels in PC3 after treatment with Etoposide.** *Panel a*: Western Blot analyses were performed at 0.5, 1 and 4 hs after treatment with Etoposide. Tubulin was used as loading control. *Panel b*: mRNA level of ABCG2 normalized to 18S. Data points represent the average of triplicate determinations (media±SD). Statistical significance (in respect to control) P values: ** < 0.01, *** < 0.001.

ABCG2 protein levels increase in a dose and time dependent manner after DNA damage induced by Etoposide (FIGURE 19, panel *a*) suggesting that also its mRNA levels could increase after DNA damage. To test this point, we performed a RT-PCR on total RNA under the same conditions and we observed that the ABCG2 mRNA levels correlate with the protein levels (FIGURE 19, panel *b*). Since the major sensor of DNA damage is ATM, the serine/threonine protein kinase that is activated by DNA double-strand breaks[58, 59], we tested the effects of the ATM inhibitor namely KU-55933[60] on ABCG2 mRNA and protein levels. FIGURE 20 shows that ABCG2 mRNA levels were not induced by etoposide in the presence of the ATM inhibitor. These data show that ATM induced by DNA damage increases ABCG2 levels.

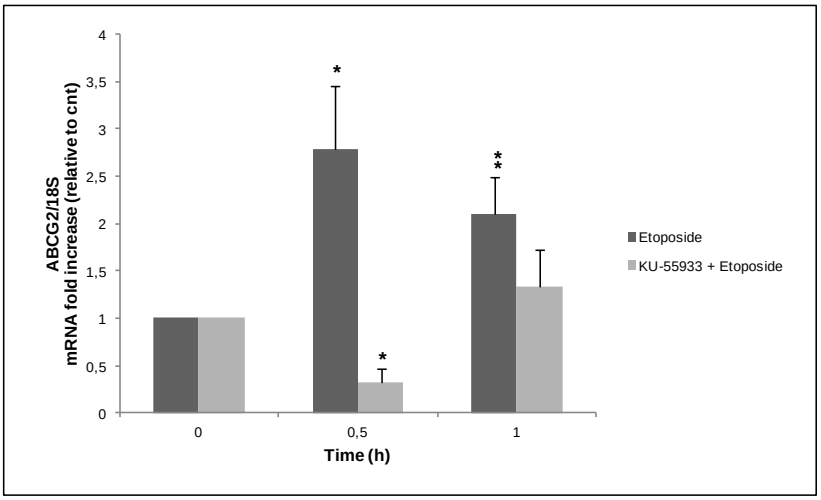

FIGURE 20. **ABCG2 expression levels in PC3 after treatment with KU-55399 and Etoposide.** mRNA level of ABCG2 normalized to 18S after treatment with Etoposide alone or with a pretreatment with KU-55399 Data points represent the average of triplicate determinations (media±SD). Statistical significance (in respect to control) P values: * < 0.05; ** < 0.01.

5. DISCUSSION

In this work, we analyze the molecular mechanism of the signals induced by 5-ALA/PDT leading to cell death by using several cell lines, with or without p53. The effects we describe are not dependent on p53 status, although stress response and DNA damage are tightly controlled by p53.

5.1 p53 STATUS DOES NOT AFFECT PDT-INDUCED CELL DEATH

In both cell lines mentioned above, 5-ALA/PDT is able to reduce cell viability. Although A549 cell line ($p53^{+/+}$) required lower doses of light fluences compared to H1299 ($p53^{-/-}$) to succumb, cell cycle profiles of A549 cells surviving 5-ALA/PDT were almost unaffected. By contrast, significant alterations of cell cycle profile were present in H1299 ($p53^{-/-}$) cell line, where is evident that cells succeeded in escaping G_1 phase but stopped cycling because were arrested in S phase. The two cell line are both NSCLC cell lines and differ only for p53 status. These data suggest that the presence or the absence of p53 may be relevant. In fact, in A549, p53 may promote a cell cycle arrest in order to repair DNA, damaged by PDT. This does not happen in H1299 due to loss of p53. To prove that p53 was responsible of such different responses, we analyzed two other cell lines that differ for p53 status. We selected two clones derived from the same cell line, HCT116 wild type ($p53^{+/+}$) and its counterpart HCT-116 $p53^{-/-}$ (knock out). As for the first two cell lines, 5-ALA/PDT affected cell viability and HCT-116 ($p53^{-/-}$) required higher light doses to undergo death. However, both cell lines present cell cycle alterations, independently of p53 status, suggesting that p53 status does not profoundly influence the sensitivity or resistance to PDT. In order to confirm such hypothesis, we selected a fifth cell line, PC3 cells, constitutively p53 null. This cell line shows, after 5-ALA/PDT, the same behavior of A549, that are, conversely, p53 positive.

Cell cycle alterations are strong signs of DNA damage than it is possible that 5-ALA/PDT, in more sensitive cell line, can be able to cause DNA damage. In order to confirm the nuclear involvement, we analyzed directly an important mark of DNA damage, phospho-γ-H2AX. We assessed the levels of phosphorylation of serine 139 in γ-H2AX histone (cytofluorimetry) and the formation of comets (comet assays), both indicators of DNA damage and replication stress[46, 52, 53]. In cells that show cell cycle profile alterations, H1299 and HCT-116 cell lines ($p53^{+/+}$ and $p53^{-/-}$), there is also an increase in the phosphorylation of histone γ-H2AX, a clear

sign of the occurrence double strand breaks at a chromatinic level and then of activation of checkpoints proteins aimed to the cell cycle arrest and DNA repair. Also, the Comet Assay analysis showed the occurrence of DNA comets, further confirming the DNA damage PDT-mediated. On the other hand, the two cell lines that did not present cell cycle alterations (A549 and PC3) showed no significant increase of γ-H2AX phosphorylation level and no comet formation, coherently with the absence of DNA damage and cell cycle alterations.

These data demonstrate that 5-ALA/PDT is able to cause DNA damage in sensitive cell lines and that p53 status is not relevant for resistance or sensitivity to 5-ALA/PDT.

5.2 ABCG2 ACTIVITY INDUCES RESISTANCE TO PDT

DNA damage may be triggered by PpIX accumulation especially in the perinuclear region and it may be not significant in cells that rapidly remove PpIX from cytoplasm. PpIX accumulation is regulated by several factors that are involved in its uptake and metabolism or in the management of its intermediates and biosynthesis[61, 62]. Despite p53 status, all five cell lines are able to uptake and metabolize 5-ALA in PpIX. This is confirmed by its characteristic emission fluorescence spectrum and by confocal microscopy images collected. Thanks to PpIX spontaneous fluorescence, such images give also important information about its localization inside the cell before and after the treatment.

Recently, it has been described that ATP binding cassette (ABC) transporters, in particular ABCG2, mediate not only the efflux of several drugs[33, 63] but also PpIX, causing resistance to PDT[36] and altering its outcome[32, 37]. ABCG2, extruding PpIX (and porphyrins in general[68]), confers cell resistance to several treatments and promotes cells survival during stress conditions.

It is known that ABCG2 expression correlates with low PpIX accumulation after 5-ALA administration[47 64]. On the basis of such evidences, we decided to analyze the expression levels of ABCG2 in our five cell lines and we found that ABCG2 expression negatively correlates with DNA injury PDT-mediated. In fact, H1299 and both HCT116 clones express low level of this protein while A459 and PC3 (that do not show clear signs of DNA damage) express high levels of this membrane transporter. Some inhibitors of ABCG2 are known and, among these, Ko143 is considered a strong inhibitor (although not highly specific at high

concentrations) that promotes PpIX accumulation[47]. This inhibitor may be able to reverse the resistance of cells to 5-ALA/PDT. In fact, after the administration of Ko143 and 5-ALA/PDT exposure, A549 and PC3 cell lines show clear signs of DNA damage.
To prove that, we compared the cellular PpIX localization in two cell lines, H1299 and PC3, that are p53 null, but differ with regard to ABCG2 expression. Both cell lines are able to internalize and metabolized 5-ALA to PpIX but PpIX distribution different because it appeared mostly perinuclear in H1299 (ABCG2 negative), and largely cytoplasmic in the PC3 cells (ABCG2 positive). They also had operative extrusion systems for PpIX because the fluorescence emission became fade during the time, if not exposed to irradiation. The exposure to light produced different effects: the PC3 cells showed 6 hours later PDT a residual fluorescence in the cytoplasm; at variance, after 6 hours from irradiation, in the H1299 cells was still present an evident PpIX fluorescent signal. The different behavior could be attributed to the activity of ABCG2, because PC3 cells, treated with the inhibitor Ko143, become no more able to extrude PpIX outside the cell .

On the basis of such evidences, we conclude that the resistance or the sensitivity of the cell lines indicated are dependent on the levels of ABCG2.

5.3 ATM INDUCES ABCG2

ABCG2, if inhibited or absent, amplifies DNA damage induced by 5-ALA/PDT, but it seems to be also activated by general DNA damage. Our experiments with KU-55399, the ATM inhibitor, or Etoposide, a drug that induces DNA damage and activates ATM, show clearly that ATM activates ABCG2 transcription because, when it is inhibited, it decreases ABCG2 mRNA levels. ROS by them selves are not as efficient as Etoposide probably because the damage and ATM activation are limited.

In conclusion, the data shown above identify a novel target to manipulate the resistance of cancer cells to PDT and suggest a mechanism of action underlying resistance of cells to a great variety of molecules used in chemotherapy.

6. CONCLUSIONS

The data presented suggest that ABCG2 expression influences the response to 5-ALA/PDT induced damage. In fact when its activity was inhibited, DNA was damaged by PDT. When PpIX can accumulate non only in the cytoplasm but also in the perinuclear area because its extrusion is inhibited, the nucleus becomes more sensitive to ROS generated by PpIX photoactivation and DNA is more susceptible to injury. DNA damage is the final effect of ROS propagation since it occurs 6 hours after irradiation, a time frame sufficient for PpIX to re-localize within the cell when ABCG2 is inactive.

The occurrence of DNA damage may represent an improvement for 5-ALA/PDT clinical applications.

Taking together, the present observations not only provide new information on the effectiveness of 5-ALA/PDT but also indicate a potential way to shift PDT from a palliative to a more effective tool in cancer therapy

Moreover, ABCG2 expression is induced not only by ROS, but also by DNA damage itself. In particular, its expression is enhanced by ATM activation since ATM inhibition reduces significantly ABCG2 levels.

These data highlight a complex interaction between DNA damage checkpoints and ABCG2 levels, which can be extended to other DNA damaging agents.

7. ACKNOWLEDGEMENTS

I would like to thank *Prof. Giuseppe Palumbo* that introduced me in the beautiful world of Photobiology giving me the possibility to work in his laboratory. Thanks for the energy and the time dedicated to me during these years and for the professional and constructive time.

A very special thanks to *Dr. Ilaria Postiglione,* the best teacher I could ever have side by side in the lab. Thanks for giving me a critical point of view inside and outside the lab. Thanks for helping me every time and everywhere. Thanks for making me more stubborn (in a positive way), for giving me independence (and independent) and for teaching me that (if I want) I know how to be stronger than I thought.

I would like to thank *Prof. Vittorio Enrico Avvedimento* for giving me the possibility to continue my PhD project and the opportunity to improve my knowledge by attending its laboratory.

Thanks to *Dr. Antonio Pezone* for stimulating me into deeper and deeper scientific questions and for helping me with recent aspects of my research.
Thanks to the other "senior" of VEA's lab, *Dr. Giusi Russo, Dr. Rosaria Landi* and *Dr. Jacopo Dolcini* for their useful advices in the lab and for the joyful moments spent together.
Thanks to *Dr. Mariarosaria De Rosa* for sharing with me the last year of PhD, working together side by side.
Thanks to *Dr. Giuliana La Rosa* for her happiness that welcomed me every morning.
A special thanks to *Dr. Alfonso Tramontano* for his immense patience.

Thanks to *Dr. Chiara Allocca* for her constant support during these years.

Thanks to *Dr. Amy Soriano* for still being by my side.

Thanks to *DSB group,* without them I would never get so far.

Thanks to *my parents* and to *my family* for their unreserved support.

Thanks to *my Gruppo Storico* for being always my biggest fans.

Thanks to *Elena, Cristina* and *Mila* for their constant presence in my life

Thanks to *my little Chiara*, for the breath of freshness and hope that she always carries with her.

A very special thanks to my *Sma* for his unconditional love, despite everything.

8. REFERENCES

[1] Dolmans DE, Fukumura D, Jain RK. (2003). Photodynamic therapy for cancer. *Nat Rev Cancer*. 3(5), 380-7.

[2] Dougherty TJ. (1992) Photochemistry in the treatment of cancer. *Adv. Photochem.* 17, 275–311.

[3]Dougherty TJ, Potter WR. (1991) Of what value is a highly absorbing photosensitizer? *J. Photochem. Photobiol. B: Biol.* 8, 233–234.

[4] Moan J, Berg K. (1991) The photodegradation of porphyrins in cells can be used to estimate the lifetime of singlet oxygen. *Photochem. Photobiol*. 53, 549–553

[5] Ackroyd R, Kelty C, Brown N, Reed M. (2001) The history of photodetection and photodynamic therapy. *Photochem Photobiol.* 74(5), 656-69.

[6]Josefsen LB, Boyle RW.(2008) Photodynamic therapy and the development of metal-based photosensitisers. *Met Based Drugs.* 2008, 276109. doi: 10.1155/2008/276109.

[7] Dougherty TJ, Grindey GB, Fiel R, Weishaupt KR, Boyle DG. (1975) Photoradiation therapy. II. Cure of animal tumors with hematoporphyrin and light. *J. Natl Cancer Inst.* 55, 115–121.

[8] Dougherty TJ. (1983) Hematoporphyrin as a photosensitizer of tumors. *Photochem. Photobiol.* 38, 377–379.

[9] Macdonald IJ, Dougherty TJ. (2001), Basic principles of photodynamic therapy. *J. Porphyrins Phthalocyanines*, 5, 105–129. doi:10.1002/jpp.328.

[10] Foote CS (1991) Definition of type I and type II photosensitized oxidation. *Photochem. Photobiol.* 54, 659.

[11] Hatz S, Lambert JD, Ogilby PR. (2007) Measuring the lifetime of singlet oxygen in a single cell: addressing the issue of cell viability. *Photochem. Photobiol. Sci.* 6, 1106–1116.

[12] Allison RR, Downie GH, Cuenca R, Hu XH, Childs CJ, Sibata CH. (2004) Photosensitizers in clinical PDT. *Photodiagnosis Photodyn Ther*. 1, 27-42. doi: 10.1016/S1572-1000(04)00007-9.

[13] Shemin D: The biosynthesis of porphyrins. The Harvey Lectures, Vol 50, Ser L. New York, NY, Academic, 1956, p 258

[14] Peng, Q., Berg, K., Moan, J., Kongshaug, M. and Nesland, J. M. (1997), 5-Aminolevulinic Acid-Based Photodynamic Therapy: Principles and Experimental Research. Photochemistry and Photobiology, 65: 235–251. doi:10.1111/j.1751-1097.1997.tb08549.x

[15] Collaud S, Juzeniene A, Moan J, Lange N. (2004) On the selectivity of 5-aminolevulinic acidinduced protoporphyrin IX formation. *Curr. Med. Chem. Anticancer Agents*, 4, 301-316.

[16] Hinnen P, de Rooij FW, van Velthuysen ML, Edixhoven A, van Hillegersberg R, Tilanus HW. et al. (1998) Biochemical basis of 5-aminolaevulinic acid-induced protoporphyrin IX accumulation: A study in patients with (pre)malignant lesions of the oesophagus. *Br. J. Cancer* 78, 679-682.

[17] Ohgari Y, Nakayasu Y, Kitajima S, Sawamoto M, Mori H, Shimokawa O, et al. (2005) Mechanisms involved in delta-aminolevulinic acid (ALA)-induced photosensitivity of tumor cells: Relation of ferrochelatase and uptake of ALA to the accumulation of protoporphyrin. *Biochem. Pharmacol.* 71, 42-49.

[18] Stout DL, Becker FF. (1990) Heme synthesis in normal mouse liver and mouse liver tumors. *Cancer Res.* 50, 2337-2340.

[19] Kennedy JC, Pottier RH, Pross DC. (1990) Photodynamic therapy with endogenous protoporphyrin IX: Basic principles and present clinical experience. *J. Photochem. Photobiol. B* 6, 143-148.

[20] Pariser DM, Lowe NJ, Stewart DM, et al. (2003) Photodynamic therapy with topicalmethylaminol evulinate for actinic keratosis: results of a prospective randomized multicenter trial. *J Am Acad Dermatol* 48,227-32.

[21] Waidelich R, Beyer W, Knuchel R, et al. (2003) Whole bladder PDT with 5-ALA and a white light source. *Urology*, 61, 332-7.

[22] Teng L, Nakada M, Hayashi Y, Yoneyama T, Zhao SG, Hamada JI (2013) Current Applications of 5-ALA in Glioma Diagnostics and Therapy . from: "Clinical Management and Evolving Novel Therapeutic Strategies for Patients with Brain Tumors", ISBN 978-953-51-1058-3, DOI: 10.5772/52428.

[23] Namikawa T, Yatabe T, Inoue K, Shuin T, Hanazaki K. (2015) Clinical applications of 5-aminolevulinic acid-mediated fluorescence for gastric cancer. *World J Gastroenterol.* 21, 8769–8775. doi:10.3748/wjg.v21.i29.8769.

[24] Cantisani C, Paolino G, Faina V, Frascani F, Cantoresi F, Bianchini D et al. (2014) Overview on Topical 5-ALA Photodynamic Therapy Use for Non Melanoma Skin Cancers *Int. J. Photoenergy* 2014, 304862, http://dx.doi.org/10.1155/2014/304862.

[25] Buytaert E, Dewaele M, Agostinis P. (2007) Molecular effectors of multiple cell death pathways initiated by photodynamic therapy. *Biochim Biophys Acta* 1776, 86-107.

[26] Oleinick NL, Morris RL, Belichenko I. (2002) The role of apoptosis in response to photodynamic therapy: what, where, why, and how. *Photochem Photobiol Sci.* 1, 1-21.

[27] El-Hussein A, Harith M, Abrahamse H. (2012) Assessment of DNA Damage after Photodynamic Therapy Using a Metallophthalocyanine Photosensitizer. *Int J Photoenergy* 2012, 1-10. doi: 10.1155/2012/281068.

[28] Tada-Oikawa S, Oikawa S, Hirayama J, Hirakawa K, Kawanishi, S (2009) DNA Damage and Apoptosis Induced by Photosensitization of 5,10,15,20-Tetrakis (N-methyl-4-pyridyl)-21H,23H-porphyrin via Singlet Oxygen Generation. *Photochem. Photobiol.* 85, 1391.

[29] Wiseman H, Halliwell B (1996) Damage to DNA by Reactive Oxygen and Nitrogen Species: Role in Inflammatory Disease and Progression to Cancer. *Biochem. J.* 313, 17-29.

[30] Doyle LA, Yang W, Abruzzo LV, Krogmann T, Gao Y, Rishi AK, et al. (1998) A multidrug resistance transporter from human MCF-7 breast cancer cells. *Proc. Natl. Acad. Sci. U S A.* 95(26), 15665-70.

[31] Mo W, Zhang JT. (2012). Human ABCG2: structure, function, and its role in multidrug resistance. *Int J Biochem Mol Biol.* 3, 1-27.

[32] Ishikawa T, Nakagawa H, Hagiya Y, Nonoguchi N, Miyatake S, Kuroiwa T (2010) Key Role of Human ABC Transporter ABCG2 in Photodynamic Therapy and Photodynamic Diagnosis. *Adv. Pharmacol. Sci.* 2010, 587306. doi: 10.1155/2010/587306.

[33] Knutsen T, Rao VK, Ried T, Mickley L, Schneider E, Miyake K, et al. (2000) Amplification of 4q21-q22 and the MXR gene in independently derived mitoxantrone-resistant cell lines. *Genes Chromosomes Cancer.* 27, 110-116.

[34] Robey RW, Medina-Perez WY, Nishiyama K, Lahusen T, Miyake K, Litman T, et al. (2001) Overexpression of the ATP-binding cassette half-transporter, ABCG2 (Mxr/BCrp/ABCP1), in flavopiridol-resistant human breast cancer cells. *Clin Cancer Res.* 7, 145-152.

[35] Zhou S, Zong Y, Ney PA, Nair G, Stewart CF, Sorrentino BP (2005) Increased expression of the Abcg2 transporter during erythroid maturation plays a role in decreasing cellular protoporphyrin IX levels. *Blood*, 105(6) 2571-2576.

[36] Kim JH, Park JM, Roh YJ, Kim IW, Hasan T, Choi MG (2015) Enhanced efficacy of photodynamic therapy by inhibiting ABCG2 in colon cancers. *BMC Cancer*, 15, 504. doi: 10.1186/s12885-015-1514-4.

[37] Robey RW, Steadman K, Polgar O, Bates SE (2005) ABCG2-mediated transport of photosensitizers: potential impact on photodynamic therapy. *Cancer Biol. Ther*. 4, 187-194.

[38] Jonker JW, Buitelaar M, Wagenaar E, Van Der Valk MA, Scheffer GL, Scheper RJ, et al., (2002) The breast cancer resistance protein protects against a major chlorophyll-derived dietary phototoxin and protoporphyria, *Proc. Natl. Acad. Sci. USA*, 99, 15649–15654.

[39] Akhlynina TV, Jans DA, Rosenkranz AA, Statsyuk NV, Balashova IY, Toth G, et al (1997) Nuclear Targeting of Chlorin e6 Enhances its Photosensitizing Activity. *J. Biol. Chem.* 272, 328-331.

[40] Bunz F, Hwang PM, Torrance C, Waldman T, Zhang Y, Dillehay L, et al. (1999) Disruption of p53 in human cancer cells alters the responses to therapeutic agents. *J. Clin. Invest.* 104, 263–269.

[41] Barron GA, Moseley H, Woods JA (2013) Differential sensitivity in cell lines to photodynamic therapy in combination with ABCG2 inhibition. *J. Photochem. Photobiol. B.* 126, 87-96.

[42] Weidner LD, Zoghbi SS, Lu S, Shukla S, Ambudkar SV, Pike VW, et al. (2015) The Inhibitor Ko143 Is Not Specific for ABCG2. *J. Pharmacol. Exp. Ther.* 354(3), 384-393. doi: 10.1124/jpet.115.225482.

[43] Postiglione I, Chiaviello A, Aloj SM, Palumbo G. (2013) 5-aminolaevulinic acid/photo-dynamic therapy and gefitinib in non-small cell lung cancer cell lines: a potential strategy to improve gefitinib therapeutic efficacy. *Cell Prolif.* 46, 382-395.

[44] Egli RJ, Di Criscio A, Hempfing A, Schoeniger R, Ganz R, Hofstetterì W et al. (2008) In vitro resistance of articular chondrocytes to 5-Aminolaevulinic acid based photodynamic therapy. *Lasers Surg. Med.* 40, 282–290.

[45] Wild L, Burn JL, Reed MW, Brown NJ (1997) Factors affecting aminolaevulinic acid-induced generation of protoporphyrin IX. *Brit. J. Cancer*, 76. 705-712.

[46] Lovell DP, Omori T (2008) Statistical issues in the use of the comet assay. *Mutagenesis*, 23, 171-182.

[47] Kobuchi H, Moriya K, Ogino T, Fujita H, Inoue K, Shuin T, et al. (2012) Mitochondrial localization of ABC transporter ABCG2 and its function in 5-aminolaevulinic acid-mediated protoporphyrin IX accumulation. *PLoS One,* 7(11), e50082.

[48] Chiaviello A, Paciello I, Postiglione I, Crescenzi E, Palumbo G (2010) Combination of photodynamic therapy with aspirin in human-derived lung adenocarcinoma cells affects proteasome activity and induces apoptosis. *Cell Prolif.* 43, 480–493.

[49] Bradford M (1976) A rapid and sensitive method for the quantitation of microgram quantities of protein utilizing the principle of protein dye binding. *Anal. Biochem.* 72, 248–254.

[50] Laemmli UK (1971) Cleavage of structural proteins during the assembly of the head of bacteriophage T4. *Nature*, 227, 680–685.

[51] Livak KJ, Schmittgen TD (2001) Analysis of relative gene expression data using real-time quantitative PCR and the 2(-DeltaDelta C(T)) Method Methods 25(4):402–408. pmid:11846609

[52] Rogakou EP, Pilch DR, Orr AH, Ivanova VS, Bonner WM (1998) DNA double-stranded breaks induce histone H2AX phosphorylation on serine 139. *J. Biol. Chem.* 273, 5858–5868.

[53] Redon C, Pilch D, Rogakou E, Sedelnikova O, Newrock K, Bonner W (2002) Histone H2A variants H2AX and H2AZ. *Curr. Opin. Genet. Dev.*12, 162-169.

[54] Scharenberg CW, Harkey MA, Torok-Storb B (2002) The ABCG2 transporter is an efficient Hoechst 33342 efflux pump and is preferentially expressed by immature human hematopoietic progenitors. *Blood*, 99, 507-512.

[55] Ma Y, Liang D, Liu J, Axcrona K, Kvalheim G, Stokke T, et al. (2011) Prostate cancer cell lines under hypoxia exhibit greater stem-like properties. *PLoS One*, 6, e29170.

[56] Fridovich I. (1978) The biology of oxygen radicals. *Science*, 201, 875-80.

[57] Baldwin EL, Osheroff N. (2005) Etoposide, topoisomerase II and cancer. *Curr Med Chem Anticancer Agents*, 5, 363-72.

[58] Abraham RT (2001) Cell cycle checkpoint signaling through the ATM and ATR kinases. *Genes dev.* 15, 2177–2196

[59] Matt S, Hofmann TG. (2016) Cell The DNA damage-induced cell death response: a roadmap to kill cancer cells. *Mol Life Sci.* 73, 2829-50. doi: 10.1007/s00018-016-2130-4.

[60] Ding J, Miao ZH, Meng LH, Geng MY. (2006) Emerging cancer therapeutic opportunities target DNA-repair systems. Trends Pharmacol Sci. 27, 338-44.

[61] Frank J, Lornejad-Schäfer MR, Schöffl H, Flaccus A, Lambert C, Biesalski HK (2007) Inhibition of heme oxygenase-1 increases responsiveness of melanoma cells to ALA-based photodynamic therapy. *Int. J. Oncol.* 31, 1539-1545.

[62] Krishnamurthy P, Xie T, Schuetz JD (2007) The role of transporters in cellular heme and porphyrin homeostasis. *Pharmacol. Ther.* 114, 345-358.

[63] Bakhsheshian J, Hall MD, Robey RW, Herrmann MA, Chen J, Bates SE et al. (2013) Overlapping Substrate and Inhibitor Specificity of Human and Murine ABCG2. *Drug Metab Dispos.* 41(10): 1805–1812.doi: 10.1124/dmd.113.053140).

[64] Palasuberniam P, Yang X, Kraus D, Jones P, Myers KA, Chen B (2015) ABCG2 transporter inhibitor restores the sensitivity of triple negative breast cancer cells to aminolevulinic acid-mediated photodynamic therapy. *Sci. Rep.* 5, 13298. doi: 10.1038/srep13298.